UNIVERSIDADE ESTADUAL PAULISTA
INSTITUTO DE GEOCIÊNCAS E CIÊNCAS EXATAS
CAMPUS DE RIO CLARO

Isotopic and Elemental Determination of Lead in Particulate Matter in the Cities of Goiânia (GO) and Rio Claro (SP) using ICP-MS technique

Hendryk Gemeiner

Dissertação de Mestrado apresentada ao Instituto de Geociências e Ciências Exatas do Campus de Rio Claro, da Universidade Estadual Paulista - "Júlio de Mesquita Filho" como parte dos requisitos para obtenção do título de Mestre em Geociências e Meio Ambiente.

Orientador: Prof. Dr. Amauri Antonio Menegário
Co-Orientador: Prof. Dr. Didier Gastman

Rio Claro - SP
Setembro de 2016

551.9 Gemeiner, Hendryk
G322i Isotopic and elemental determination of lead in particulate matter in the cities of Goiânia (GO) and Rio Claro (SP) using ICP-MS technique / Hendryk Gemeiner. - Rio Claro, 2016
80 f. : il., figs., gráfs., tabs., fots., mapas

Dissertação (mestrado) - Universidade Estadual Paulista, Instituto de Geociências e Ciências Exatas
Orientador: Amauri Antonio Menegário
Coorientador: Didier Gastmans

1. Geochemistry. 2. Lead (Pb). 3. Lead isotope ratio. 4. Particulate matter. 5. ICP-MS. I. Título.

Ficha Catalográfica elaborada pela STATI - Biblioteca da UNESP
Campus de Rio Claro/SP

UNIVERSIDADE ESTADUAL PAULISTA
INSTITUTO DE GEOCIÊNCAS E CIÊNCAS EXATAS
CAMPUS DE RIO CLARO

Isotopic and Elemental Determination of Lead in Particulate Matter in the Cities of Goiânia (GO) and Rio Claro (SP) using ICP-MS technique

Hendryk Gemeiner

Dissertação de Mestrado apresentada ao Instituto de Geociências e Ciências Exatas do Campus de Rio Claro, da Universidade Estadual Paulista - "Júlio de Mesquita Filho" como parte dos requisitos para obtenção do título de Mestre em Geociências e Meio Ambiente.

Comissão Examinadora

Prof. Dr. Amauri Antonio Menegario
Orientador – CEA/UNESP - Rio Claro/SP

Profa. Dra. Veridiana Teixeira de Souza Martins
IG – USP – São Paulo/SP

Dra. Juliana Aparecida Galhardi
CEA/UNESP – Rio Claro/SP

Conceito: Aprovado

Rio Claro - SP
13 de Setembro de 2016

Isotopic and Elemental Determination of Lead in Particulate Matter in the Cities of Goiânia (GO) and Rio Claro (SP) using ICP-MS technique

List of figures

List of tables

Abstract

The toxic metal lead (Pb) can be harmful to human health in various manners, but is also considered as a distinguished tracer of environmental pollution, since the relative abundance of its four stable isotopes with the atomic masses of 204, 206, 207 and 208 varies with the emission source. This study is focused on the lead concentrations and isotope ratios in the particulate matter of the Brazilian cities of Goiânia (GO) and Rio Claro (SP), in order to determine the main Pb pollution sources. Particulate matter samples were collected on clean Teflon filters during the rainy and dry season between 2014 and 2016 on the campus of the State University of São Paulo (UNESP) in Rio Claro city and in the centre of Goiânia city near main roads with a high traffic volume. The Pb concentrations as well as the $^{206}Pb/^{207}Pb$ and $^{208}Pb/^{207}Pb$ stable isotope ratios of the particulate matter samples were analysed by Inductively-Coupled Plasma Mass Spectrometry. To apply this analytical technique successfully, it was necessary to optimize parameters in case of acquisition time, detector dead time and mass discrimination, which affect the measurement accuracy and precision. Results showed that lead concentrations in Goiânia were different between rainy and dry season. In Goiânia, Pb concentrations showed higher values in dry season than in rainy season, while Pb concentrations were more similar in both sampling periods in Rio Claro. Back trajectories were analysed with the HYSPLIT model to investigate associations between Pb concentration levels and the direction of incoming air masses. However, the comparison of the obtained $^{206}Pb/^{207}Pb$ and $^{208}Pb/^{207}Pb$ isotope ratios data with data of potential Pb sources from previous studies indicated that gasoline may be considered as main Pb sources in the particulate matter of Goiânia and Rio Claro. Pb isotope ratios in Goiania were slightly different between dry and rainy season, while in Rio Claro, $^{206}Pb/^{207}Pb$ isotope ratios showed markedly higher values in dry season than in rainy season. Hence, Pb in Rio Claro in dry season also seems to be influenced by industrial emissions. These assumptions were supported by the calculation of $^{208}Pb/^{206}Pb$-$^{207}Pb/^{206}Pb$ diagrams and the contribution factor of Pb coming from gasoline by applying binary mixing equations.

Key words: Lead, Lead isotope ratio, Particulate Matter, ICP-MS

Resumo

O metal tóxico de chumbo (Pb) pode ser prejudicial para a saúde humana em várias maneiras, mas também pode ser utilizado como um traçador da poluição ambiental, porque a abundância relativa dos seus quatro isótopos estáveis de massas 204, 206, 207 e 208 conhecidos varia de acordo com a fonte de emissão. Este estudo é focado nas concentrações de chumbo e nas razões isótopicas de material particulado das cidades brasileiras de Rio Claro (SP) e Goiânia (GO), a fim de determinar as principais fontes de poluição por Pb. Amostras de material particulado foram recolhidas em filtros de teflon limpos, durante a estações chuvosa e seca entre anos de 2014 e 2016 na UNESP – Campus de Rio Claro e no centro de Goiânia nas proximidades das estradas principais com um grande volume de tráfego. As concentrações de Pb e as razões isótopicas estáveis de $^{206}Pb/^{207}Pb$ e $^{208}Pb/^{207}Pb$ das amostras de material particulado foram analisadas por ICP-MS. Para aplicar esta técnica, foi necessário otimizar os parâmetros como o tempo de aquisição, tempo morto de detector e discriminação de massa, que afetam a exatidão da medida e precisão. Em Goiânia, as concentracões de Pb exibiram valores mais elevados na estação seca do que na estação chuvosa, enquanto as concentracões de Pb foram similares em ambas as campanhas de amostragem em Rio Claro. Trajetórias de volta do modelo HYSPLIT foram analisadas, a fim de investigar-se associações entre os níveis de Pb e as direções das massas de ar. Entretanto, a comparação entre os valores das razões isótopicas $^{206}Pb/^{207}Pb$ e $^{208}Pb/^{207}Pb$ e os dados das fontes potenciais de Pb a partir de estudos prévios indicaram que a gasolina pode ser considerada como a principal fonte de Pb para o material particulado em Goiânia e Rio Claro. As razões isótopicas de Pb em Goiânia foram levemente distintas entre os períodos seco e chuvoso, enquanto em Rio Claro as razões $^{206}Pb/^{207}Pb$ exibiram de forma marcante valores mais elevados na estação seca. Portanto, o Pb em Rio Claro na estacão seca tambem aparenta ser influenciado por emissões industriais. Tais considerações são corroboradas pelo cálculo do fator de contribuição de Pb advindo da gasolina ao aplicar-se equações de mistura binária.

Palavras-chave: Razão isotópica de chumbo, Material Particulado, ICP-MS

Contents

1 Introduction and Objectives

Air pollution caused by particulate matter produces a plurality of harmful effects on human health, as statistical associations in previous studies between health effects and particle concentration in the air, especially fine particles with an aerodynamic diameter of 10 µm (PM_{10}), are showing (Schwartz et al., 1996; Pope, 2002). Particles larger than 10 µm can be filtered out in the human nasopharynx and trachea, but smaller particles penetrate deep into the lungs, may even getting into the bloodstream, which results in a number of health problems in extremely serious conditions. Furthermore, particulate matter is a catalyser for reaction of gas pollutants and thus having a significant influence on the climate (Zheng et al., 2004).

On the other hand, lead is a poisonous metal, that produces adverse effects on human health in low concentrations, damaging nervous connections, especially on infants, and causing blood and brain diseases. Besides this, lead can also be used as an ambient pollution tracer, according to its four stable isotopes with the atomic masses of 204, 206, 207 and 208, which abundances depend on the emission source, known as isotopic signature. This principle has been used in a variety of ways to determine anthropogenic sources of Pb, for example in freshwater, sediments, aerosols and particulate matter (Mastral et al., 2009). For an accurate elemental and isotopic determination of lead in particulate matter, the use of appropriate analytical methods, such as Inductively Coupled Plasma Mass Spectrometry (ICP-MS), is required, due to its high detection capability and its ability to obtain isotopic information (EPA, 2011).

The growth of the regions of Goiânia, located in the centre of Brazil and capital of the state of Goiás, and Rio Claro, located in the south of Brazil in the middle east of the state of São Paulo, is highly connected with environmental problems like air pollution, introducing a wide range of toxic gases, vapours and particulate matter in the atmosphere, causing serious effects on human health like mentioned above. The ceramic production in Rio Claro and emissions from motor vehicles representing two of the main contaminant sources (CETESB, 2014).

1.1 Objectives

The main objective of this study is to determine and compare contents and isotope ratios of lead in particulate matter of air in the cities of Goiânia (GO) and Rio Claro (SP) in the dry and rainy season, in order to identify possible Pb emission sources in both cities.

For the city of Goiânia, it was expected that the Pb isotope ratios in particulate are related with the combustion of fossil fuels, while for the city of Rio Claro, it was assumed that the Pb isotope ratios are influenced by the burning process of the raw material in the industrial activity of the ceramic production.

Furthermore, basic methods using ICP-MS technique had to be implement previously to ensure an accurate and precise determination of Pb isotope ratios.

2 Literature Review

2.1 Particulate Matter

Air pollution is basically present as aerosols or particulate matter (PM). This particulate material is composed by solid or liquid particles in suspension, forming clusters and particles of different sizes and different degrees of toxicity and physicochemical properties. Particulate Matter can be characterized by the distribution of its particle sizes and its chemical compositions (Jacobson, 2002). It has varied chemical compositions, mainly due to the combination of fine particles with secondary pollutant gases (Godish, 1997). The particle size can vary from a few nanometres in diameter up to several micrometres. The finer particles are associated with health problems. (Wholgate et al. 1999; Pope et al. 2002; WHO 2006; Lewtas et al. 2007).

The size of particles is directly linked to their potential for causing health problems. The fine particulate matter, which consists of particles suspended in air smaller than 2.5 μm in aerodynamic diameter ($PM_{2.5}$), reaches the

bronchioles through respiration, whereas coarse particles between 2.5 and 10 µm (PM_{10}) are retained in the nostrils and nasopharyngeal tract and are subsequently eliminated from the body (Godish, 1997).

Numerous scientific studies have linked particle pollution exposure to a variety of problems, including premature death in people with heart or lung diseases, nonfatal heart attacks, irregular heartbeat, aggravated asthma, decreased lung function and increased respiratory symptoms, such as irritation of the airways, coughing or difficulty of breathing (Pope et al., 1995; Schwartz et al., 1996, Zheng et al., 2004).

Besides causing harmful effects on human health, airborne particles are pollutants that reduce visibility. Particulate matter can be carried over long distances by wind and then settle on ground or water. The effects of this settling can result in acidifying lakes and streams, changing the nutrient balance in coastal waters and large river basins, depleting the nutrients in soil, damaging sensitive forests and farm crops, and affecting the diversity of ecosystems. Moreover, it catalyses gas pollutant reactions and thus, influences the climate (Kyotani and Iwatsuki, 2002; EPA, 2015).

Some particles, known as primary particles, are emitted directly from a source, such as construction sites, unpaved roads, fields, smokestacks or fires. Others are form in complicated reactions in the atmosphere by chemicals, such as sulphur dioxides and nitrogen oxides, that are emitted from power plants, industries and automobiles. The fine particulate matter ($PM_{2.5}$) is highly connected to sources of combustion processes, like industrial chimneys, vehicle fuel and biomass burning. Chemical species commonly found in this kind of particles are nitrates, sulphates, heavy metals such as lead, organic compounds and carbon (Hopke, 1991).

2.2 Properties of Lead

Lead (Pb) is one of the chemical elements which is frequently found in particulate matter, derived from contamination sources mentioned above. It is a poisonous metal, that can cause health damages by harming nervous connections, affecting kidney functions and causing blood and brain disorders.

This is particularly a risk for young children, due to the increased sensitivity of young tissues and organs (Wang and Zhang, 2006; Mastral et al. 2009).

Having an atomic mass of 207.2, lead has four naturally occurring isotopes: ^{204}Pb (1.4%), ^{206}Pb (24.1%), ^{207}Pb (22.1%) and ^{208}Pb (52.4%). However, the ratio between the different lead isotopes vary in different geological environments, *e.g*. ^{206}Pb and ^{207}Pb are formed by the radioactive decay of ^{238}U ($T_{1/2}$ = 4.47 10^9 years) and ^{235}U ($T_{1/2}$ = 7.04 10^8 years), while ^{208}Pb is the product of the decay of ^{232}Th ($T_{1/2}$ = 1.4 10^{10} years). ^{204}Pb is the only lead isotope which is not a product of radioactive decay. Thus, the isotope ratio of lead depends on the concentration of Pb, Th and U in the starting mixture of the particular environment, the half-life of the decay process and the elapsed time of this process. Hence, every lead ore deposit shows its own characteristic lead composition, due to its age, which represents the time that the lead separated from its source rocks, and the condition of its genesis. Thus, the isotopic composition of Pb in environmental materials can be coupled with the ore bodies from which it was derived. Therefore, if each source of lead has a distinctive isotopic composition, the mixing processes of local Pb and anthropogenic inputs in the environment can be quantified by the Pb isotope ratios (Monna et al., 1995).

The isotope ratio of lead is highly representative for its origin and so can be used to identify sources of contamination in soils, sediments, water, marshes, tree trunks, marine organisms and others (Margui et al. 2007). Furthermore, the isotopic composition of lead in the atmosphere is characteristic for a particular region, mainly due to the anthropogenic emission of the element, having a relatively long atmospheric residence time of 5-10 days. Therefore, the Pb isotopic signature is considered as an ideal tool for tracing sources of atmospheric pollution (Settle and Patterson, 1991). Lead isotopes have the advantage of not being fractionated in the part of any natural chemical or biological process on the earth's surface. The environmental sources of lead vary widely and in order to use the isotopic signature as a discriminatory tool, it is necessary that the isotopic ratios are different for each source (Bellis et al., 2005).

Lead is naturally abundant in the terrestrial crust, but anthropogenic Pb

has a relatively higher abundance in the urban atmosphere than in the natural fraction, which comes from sources such as soil dust or sea salt. For a long time, one of the main lead anthropogenic sources was related to traffic emissions due to alkyl lead derivatives used as antiknock agents in gasoline, accounting for 90 percent of airborne lead pollution. In order to reduce its concentration, restrictive normatives in several countries like the USA or the European Union (Directive 98/70/EC, 2000) were established. New non-leaded gasoline with a high octane index was introduced into the market and more resistant materials in the engine industry were used, which not needed lead lubrication for its maintenance. However, lead is still introduced into the atmosphere by traffic, as the current used gasoline still possesses variable lead amounts due to its presence in the crude oil (10–300 μg l^{-1}). In contrast, the concentration of Pb in diesel emissions is usually smaller than 1 μg l^{-1} (Mastral et al., 2009).

Other anthropogenic lead sources are smelting, steel mills, incineration of residues, wood and coal combustion, resuspension of contaminated grounds and general production activities like production of paintings, chemical agents, welds, etc. (Flament et al., 2002; Widory et al., 2004).

2.3 Legislation and Standard Values for Particulate Matter and Lead

The Brazilian National Council of Environment (CONAMA) established in the Resolution No. 003 of 1990 parameters for air quality in case of PM_{10} and TSP (total suspended particles), but no regimentation exists for $PM_{2.5}$. This national resolution sets a standard for the annual geometric mean concentration of total suspend particles of 80 μg m^{-3} along with a mean concentration of 240 μg m^{-3} that should not be exceeded in more than one time per year. Whereas, for inhalable particles (PM_{10}), it is set a standard value of 50 μg m^{-3} for the arithmetic mean concentration and the mean concentration of 150 μg m^{-3} in 24 hours should not be exceeded more than one time per year (CONAMA, 1990).

A standard for lead is not included in the resolution, but was established along with $PM_{2.5}$ and PM_{10} standards by the Environmental State Company of

São Paulo (CETESB) in the Decree No. 59113/2013 (Table 1). There, the air quality standards were launched in two criteria. Intermediate goals (MI) were set up as temporary values to be achieved in stages, aiming the gradual improvement of air quality in São Paulo state, based on efforts to reduce emissions from stationary and mobile sources, in line with the principles of a sustainable development. Final standards (PF) are standards determined by the best scientific knowledge for preserving people's health as much as possible in relation to effects on human health caused by air pollution (CETESB, 2013).

Table 1: Standard values for PM_{10}; $PM_{2.5}$; TSP and Pb established by CETESB (Source: CETESB, 2013)

Pollutent	Sampling time	MI1	MI2	MI3	PF
PM_{10}	24 hours MAA[1]	120 μg m^{-3} 40 μg m^{-3}	100 μg m^{-3} 35 μg m^{-3}	75 μg m^{-3} 30 μg m^{-3}	50 μg m^{-3} 20 μg m^{-3}
$PM_{2.5}$	24 hours MAA[1]	60 μg m^{-3} 20 μg m^{-3}	50 μg m^{-3} 17 μg m^{-3}	37 μg m^{-3} 15 μg m^{-3}	25 μg m^{-3} 10 μg m^{-3}
Total suspended particles (TSP)	24 hours MGA[2]	- -	- -	- -	240 μg m^{-3} 80 μg m^{-3}
Lead	MAA[1]	-	-	-	0.5 μg m^{-3}

Meta Intermediate Stage 1 - (MI1) - concentration values of air pollutants that must be respected since 24.4.2013;
Intermediate target Stage 2 - (MI2) - concentration values of atmospheric pollutants to be subsequently adhered to MI1, which will come into force after assessments made in Stage 1, developed by technical studies submitted by the State Environmental Agency, validated by CONSEMA;
Meta Intermediate Stage 3 - (MI3) - concentration values of air pollutants that must be respected in subsequent years to MI2, and the period of validity will be set by CONSEMA, from the beginning of its term, based on the assessments carried out in Stage 2.
The final standards (PF) are applied without intermediate stages when milestones are not established, as in the case of total particulate matter and lead. For other pollutants, the final standards go into effect from the end of the MI3 term (adopted from CETESB, 2013)

Furthermore, the Decree No. 59113/2013 also established criteria for acute episodes of air pollution. The decree states the terms "Attention", "Alert" and "Emergency" in addition to exceeded concentration levels (Table 2).

Table 2: Criteria of acute episodes of air pollution for PM_{10} and $PM_{2.5}$ established by CETESB (Source: CETESB, 2013)

Parameters	Attention	Alert	Emergency
$PM_{2.5}$ ($\mu g\ m^{-3}$) – 24 h	125	210	250
PM_{10} ($\mu g\ m^{-3}$) – 24 h	250	420	500

For each measured pollutant, an index is calculated, which is a dimensionless value. Depending on the obtained ratio, the air receives a qualification, which is a score for the air quality as shown in Table 3.

Table 3: Air quality indexes for PM_{10} and $PM_{2.5}$ established by CETESB (Source: CETESB, 2013)

Quality	Index	PM_{10} ($\mu g\ m^{-3}$) 24h	$PM_{2.5}$ ($\mu g\ m^{-3}$) 24h
N1 – Good	0 – 40	0 – 50	0 – 25
N2 – Moderate	41 – 80	>50 – 100	>25 – 50
N3 – Bad	81 – 120	>100 – 150	>50 – 75
N4 – Very Bad	121 – 200	>150 – 250	>75 – 125
N5 – Miserable	>200	>250	>125

However, the World Health Organization (WHO) recommends quality standards for $PM_{2.5}$ (WHO, 2006). Currently countries like United States, the European Union countries, Canada, Mexico and others, included the monitoring of $PM_{2.5}$, considering that this particle size causes short and long-term effects on human health (WHO, 2006).

The European Union has developed a detailed legislation body which established air quality standards and health based objectives for a number of pollutants in air. These standard values are listed in Table 4.

Table 4: Standard values for PM_{10}; $PM_{2.5}$ and Pb established by the European Union (Source: Directive 2008/50/EC, 2008)

Pollutent	***Concentration***	***Averaging period***	***Permitted exceedences each year***
$PM_{2.5}$	25 μg m^{-3}	1 year	n/a
PM_{10}	50 μg m^{-3}	24 hours	35
	40 μg m^{-3}	1 year	n/a
Lead	0.5 μg m^{-3}	1 year	n/a

With the Directive 2008/50/EC, additional objectives for $PM_{2.5}$ were introduced, which target the exposure of the population to fine particles. These objectives are set at the national level and are based on the average exposure indicator (AEI). For the best assess of $PM_{2.5}$ exposures to the general population, the AEI indicator is determined as 3-year running annual mean $PM_{2.5}$ concentrations and averaged over several selected monitoring sites in urban agglomeration areas, set in urban background locations (Directive 2008/50/EC, 2008).

In the USA, the Clean Air Act requires the United States Environmental Protection Agency (EPA) to set National Ambient Air Quality Standards (NAAQS) for pollutants that are considered as harmful to public health and the environment (Table 5). The Clean Air Act differentiates two types of national ambient air quality standards. Primary standards have the aim to provide public health protection, which includes the protection of the health of "sensitive" populations such as asthmatics, elderly people and infants. Secondary standards are set with the goal to provide public welfare protection, which involves the protection against decreased visibility and damage to animals, crops, vegetation and buildings (EPA, 2015).

Table 5: Standard values for PM_{10}; $PM_{2.5}$ and Pb established by the United States Environmental Protection (Source: EPA, 2015)

Pollutant	Primary/ Secondary	Averaging time	Level	Form
$PM_{2.5}$	primary	1 year	12.0 µg m^{-3}	Annual mean, averaged over 3 years
	secondary	1 year	15.0 µg m^{-3}	Annual mean, averaged over 3 years
	primary and secondary	24 hours	35.0 µg m^{-3}	98th percentile, averaged over 3 years
PM_{10}	primary and secondary	24 hours	150.0 µg m^{-3}	Not to be exceeded more than once per year on average over 3 years
Lead	Primary and secondary	Rolling 3 month period	0.15 µg m^{-3}	Not to be exceeded

2.4 Related Studies

Several studies on atmospheric isotope ratio of lead and its application to trace air pollution sources have been realized in Europe (Monna et al., 1995; Veron 1999; Mastral et al., 2009), in North and Central America (Sturges and Barrie, 1989; Bollhöfer and Rosman, 2001; Salcedo et al., 2016) and Asia, especially in China as urbanization and rapid economic growth has led to a profound deterioration of urban air quality (Mukai et al., 1993; Zheng et al., 2004; Xu et al., 2011; Lee et al., 2015).). In contrast, just a few studies on lead isotope ratios in particulate matter were realized in Brazil.

The group of Mukai et al. (1993) was one of the first research groups, which characterized the sources of lead in the air using stable isotope ratios of lead. The group collected particulate matter of various urban sites in China, Japan, Korea, Thailand, Sri Lanka and Indonesia and analysed them for Pb isotope ratios along with materials, that were related to the source, such as coal and leaded gasoline, using ICP-MS. A high variation of the lead isotope ratios in the air was determined, as well as that these differences highly corresponded with regional differences in the lead sources. Furthermore, the group discovered, that leaded gasoline was still a primary source in several Asian

cities, having a major effect on the lead isotope ratios in the air. However, also coal combustion and industrial activity were observed as a considerable effect in Chinese and Korean cities.

In 1995, the group of Monna et al. sampled particulate matter, incinerator ashes and gasoline from urban areas in 12 French and two British cities to determine the lead isotope ratios in order to identify Pb pollution sources, using TIMS and ICP-MS. The ratios of $^{206}Pb/^{207}Pb$ in gasoline varied from 1.061 to 1.094 (mean values were 1.084 for France and 1.067 for the United Kingdom), while for industrially derived lead, ratios of $^{206}Pb/^{207}Pb$ ranged from 1.143 to 1.155. The isotopic signature of Pb of atmospheric particulate matter reflected the relative importance of each of these sources. The study depicted that lead additives (tetraethyl lead) in gasoline were typically still the main source of Pb in urban particulate matter. The importance of Pb derived gas decreased comparing to results from other sources (natural and industrial), as a result of recent environmental legislation in the European Union, which significantly limited Pb concentrations in gasoline and increased market penetration of unleaded gasoline. Furthermore, the urban Pb isotope ratios may varied considerably due to seasonal variations in sources (*e.g.* fluctuations in traffic density) and with the wind direction.

The study of Mastral et al. (2009) was focused to the concentrations of lead and its isotope ratios of PM_{10} of Zaragoza, Spain. The objective of that study was to assess the main sources of the pollution of Pb and to verify if the influence of the prohibition of leaded gasoline inside the European Union was appropriate. PM_{10} were sampled in two campaigns, the first when leaded gasoline still was permitted and the second when leaded gasoline already were prohibited. The sampling was performed with a high volume air sampler to trap PM_{10} with glass fibre filters coated with Teflon. The filters were analysed with ICP-OES (concentration of Pb) and subsequently with ICP-MS (isotope ratios of Pb), for those samples that had higher concentrations than the quantification limit of Pb. The ICP-MS analysis resulted with differences in respect of lead isotope ratios for both sampling periods, but also showing that anthropogenic sources related to industrial processes were reflected on both campaigns. The contribution of gasoline in relation to the first sampling campaign, as for the

second campaign just an insignificant contribution was determined, confirming the success of the lead policies of the European Union on the quality of the environment.

Zheng et al. (2004) evaluated Pb concentrations and Pb isotopic ratios in samples of PM_{10}, which were collected in seven monitoring locations in Shanghai, China, to investigate the characteristics of Pb isotope ratios of the local air. Several samples related to sources of cement, coal and dust from oil combustion, metallurgic powder, exhaust particles from vehicles derived from leaded gasoline, non-leaded gasoline and polluted soil were analysed for their lead content and isotope ratios and were compared to samples of local PM_{10}. The concentrations of Pb varied between 167 and 854 ng m^{-3} in seven monitored sites with an average of 515 ng m^{-3}, indicating that a high concentration of Pb remained in the air after the gradual phasing out of leaded gasoline. Isotope ratios in PM_{10} ($^{207}Pb/^{206}Pb$ = 0.86087 ± 0.0018; $^{208}Pb/^{206}Pb$ = 2.1057 ± 0.005) were clearly distinct from the exhaust particles of vehicles ($^{207}Pb/^{206}Pb$ = 0.88547 ± 0.0075; $^{208}Pb/^{206}Pb$ = 2.1457 ± 0.006). A binary mixture equation and a source apportionment based on $^{207}Pb/^{206}Pb$ ratios were used, indicating that the contribution from automotive emission to the airborne Pb amounted around 20 %.

Lee et al. (2006) published a study describing the analysis of TSP (Total Suspended Particles) in the urban and suburban areas of the two large urban centres in South China, Hong Kong and Guangzhou. TSP samples were analysed for major elements (Al, Fe, Mg and Mn), trace elements (Cd, Cr, Cu, Pb, V and Zn) and as well for their Pb isotopic composition, focusing on the isotope ratios of $^{204}Pb/^{207}Pb$, $^{206}Pb/^{207}Pb$ and $^{208}Pb/^{207}Pb$. Besides this, seven-day air mass backward trajectories, calculated by the HYSPLIT model (HYbrid Single-Particle Lagrangian Integrated Trajectory, Version 4.7), were used in that research to assess sources of heavy metals in the analysed samples, ending at height levels of 500 m, 1000 m and 1500 m above ground level (AGL). $^{206}Pb/^{207}Pb$ and $^{208}Pb/^{207}Pb$ ratios showed lower values in winter, indicating the influence of Pb from the northern inland areas of China and the Pearl River Delta region, and $^{206}Pb/^{207}Pb$ and $^{208}Pb/^{207}Pb$ ratios were lower in summer, representing the influence of Pb from the South Asian region and from marine

sources. Analysation of air mass back trajectories assumed that enrichment of heavy metals in Hong Kong and Guangzhou was highly connected with the air masses originated from northern China, reflecting the long-range transport of heavy metal contaminants from the northern inland areas of China to the South Chinese coast.

Xu et al. (2011) determined lead concentrations as well as $^{207}Pb/^{206}Pb$ and $^{208}Pb/^{206}Pb$ isotope ratios of $PM_{2.5}$ between 2007 and 2009 in the Chinese city of Xi`an in order to investigate the effects of the phasing out of leaded gasoline in 2000. $PM_{2.5}$ samples were collected every 24 hours by using pre-fired 47 mm Whatman quartz-fibre filters. The elemental analysis was conducted by Energy Dispersive X-Ray Fluorescence and the isotopic determination by Thermo Elemental X-Series ICP-MS. Pb concentrations ranged from under the detection limit to 2.631 ng m^{-3} with an annual average of 0.306 ng m^{-3}, representing a decline since the phasing out of leaded gasoline. Pb isotope ratios were significantly lower in winter (average $^{207}Pb/^{206}Pb$ ratio of 0.843 ± 0.032; $^{208}Pb/^{206}Pb$ of 1.908 ± 0.058) than in summer ($^{207}Pb/^{206}Pb$ of 0.860 ± 0.032; $^{208}Pb/^{206}Pb$ of 2.039 ± 0.057), suggesting that coal combustion was the main Pb source in winter and vehicular emission the main Pb source in summer.

The group of Lee et al. (2015) sampled particulate matter PM_{10} and $PM_{2.5}$ in the city of Daejeon, Korea, at Asian dust periods and non-Asian dust periods. Asian dust particles, transported over long distances by westerly winds in the late winter and spring seasons, influence the ambient aerosol concentrations in Korea. Samples, daily taken by high-volume air samplers (HV-1000F, Sibata Inc., Japan) using a 20 x 25 cm^2 fibre quartz filter, were evaluated on their Pb concentration along with other elements and their Pb isotope ratios. Analysis were performed by Inductively Coupled Plasma – Atomic Emission Spectrometry (ICP-AES) and a Multi-Collector Thermal Ionization Mass Spectrometer (TIMS). Obtained patterns demonstrated that monthly mean concentrations of trace elements in winter were 2 to 13 times higher than in other seasons. The Pb isotope signature in the particulate matter from the non-Asian dust period showed lower $^{206}Pb/^{207}Pb$, $^{207}Pb/^{204}Pb$, and $^{206}Pb/^{204}Pb$ ratios in the autumn, winter, and spring seasons, demonstrating that Pb isotope ratios

were highly influenced by the industrial areas of China. The higher Pb isotope ratios in the summer indicate the dilution and/or mixing effect of marine air masses from the south.

Studies of atmospheric lead in Brazil were conducted among others by Babinski et al. (2003). The group determined Pb isotope ratios from PM_{10}, collected with Teflon filters, and rain water samples at the University of São Paulo. Isotopic lead signature of particulate matter and rain water as well as possible lead sources like gasoline, soot from vehicle exhaust pipes and PM from industrial emissions were analysed by thermal ionization mass spectrometry (TIMS). It was suggested that industrial emissions were the main contribution factor for Pb in the PM_{10} samples, since the contribution of Pb in vehicular fuels was insignificant.

In the work of Mirlean et al. (2005), lead concentrations and isotope ratios in atmospheric deposits and potential lead sources in the city of Rio Grande in South Brazil were investigated. Isotope ratios of $^{206}Pb/^{207}Pb$ and $^{208}Pb/^{207}Pb$ were measured by VG-Sector Mass Spectrometer and used trace sources of atmospheric lead from different sampling locations distributed over the city.

Gioia et al. (2010) provided the first results of a study in São Paulo City, which investigated the processes that control concentrations and sources of Pb in the atmosphere. Pb concentrations and Pb isotope ratios from PM were determined by high temporal resolution (3 hours) collection and Thermal Ionization Mass Spectrometry (TIMS) analysis. Results highlighted the possible impact of a singular short-lived pollution event, present as fireworks, on the urban air quality.

Four methods for the calculation of pulse counting detector dead time for quadrupole ICP-MS were described and analysed by the group of Nelms et al. (2000), focusing on the criteria of ease of application and accuracy. While three methods were based on the measurement of $^{204}Pb/^{208}Pb$ isotope ratio, one method were based on comparison of pulse counting signals versus the corresponding analogue signals across a range of signal intensities. The most suitable method was found out as the method based on $^{204}Pb/^{208}Pb$ measurement for different Pb concentration solutions, prepared with the NIST

Standard Reference Material NBS-982, using different dead time settings. The uncertainty in the dead time result of this method yielded minor uncertainties than the other evaluated methods.

3 Materials and Methods

3.1 Sampling

Particulate matter samples were collected in the cities of Goiânia and Rio Claro during the rainy and dry season between 2014 and 2016. 32 particulate matter samples from Goiânia (16 from April/May 2014 that represent rainy season, 16 from August 2014 that represent dry season) and 24 samples from Rio Claro (eight from July 2015 that represent dry season, 16 from December, February, March 2015/2016 that represent rainy season) were gathered. To sample particulate matter, a low volume sampler of the type STACKER, which contains a filter holder device was used. This device was connected to a diaphragm pump at the entrance and thus capturing particulate matter with a clean Teflon filter (Figure 1). These filters were Fluoropore^{TM} membrane filters of the type PTFE with a diameter of 47 mm and a pore diameter of 0.22 µm. The entrance and the AFG device were connected to a diaphragm pump, having a volume meter and maintaining an airflow of about 40 m³ per day in Goiânia and 30 m³ per day in Rio Claro. (Castanho and Artaxo, 2001)

The sampling time was 24 (Goiania samples, July 2015 samples from Rio Claro) and 48 hours (rainy season samples from Rio Claro). Sampling time of 48 hours in rainy time was chosen in order to accumulate higher amounts of particulate matter and therefore obtain higher precisions at the elemental and isotopic determination of lead, as in rainy season markedly lower amounts of particulate matter were recorded. All filter membranes were weighed (Figure 2) before and after collection in order to obtain the mass of the particulate matter.

Figure 1: Photograph of the low volume sampler STACKER (left) and the integrated filter holder device with Teflon filter (right) for particulate matter sampling

3.2 Sample Digestion

The sample digestion method was adopted from Method IO-3.1: "Selection, Preparation and Extraction of Filter Material" (Compendium of Methods for the Determination of Inorganic Compounds in Ambient Air, U.S. EPA, 1999). For each filter, digestion was realized in 10 mL of aqua regia at a concentration of 22.3 % (v v^{-1}) in a microwave tube (Figure 2) using the microwave digester Speedwave®four by BERGHOF with the parameter settings as shown in Table 6.

Table 6: Parameter settings of Speedwave®four by BERGHOF for the digestion of the particulate matter samples

Steps	Temperature	Time	Ramp	Power	Pressure
1	140 °C	10 min	5 min	45 %	35 bar
2	160 °C	10 min	5 min	45 %	40 bar
3	200 °C	5 min	5 min	45 %	35 bar

The standard solutions were prepared on the basis of the certified solid monoelemental standard SRM 981 by the National Institute of Standards & Technlogy (NIST) containing 1 g of Pb with a purity of 99,9+ %. The concentrations of aqua regia in the standards and solutions after the digestion in the microwave digester were 5.3 % (v v^{-1}).

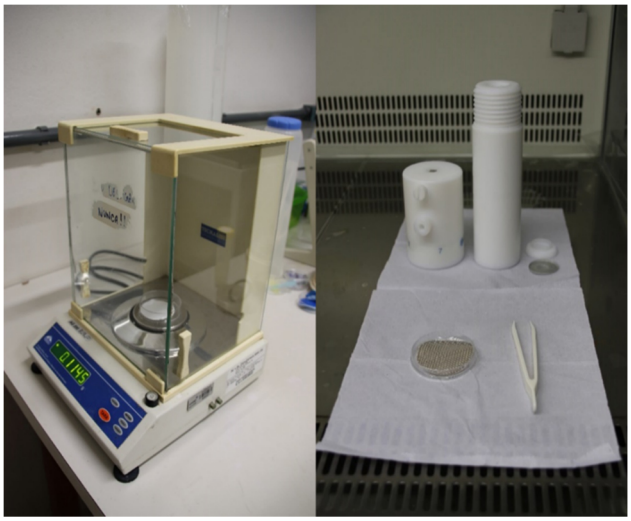

Figure 2: Gravimetric measurement of Teflon filter before sampling (left), filter with sampled particulate matter before digestion in front of microwave tube (right)

The quantification of Pb requires the use of appropriate rooms, properly decontaminated material and ultrapure reagents. To mitigate any lead interference, all decontamination procedures and sample preparations were realized under an exhaust hood and a laminar flow hood. All solutions were prepared with analytical grade chemicals, bidestillated acids below the boiling temperature and ultrapure water (18 MΩ cm). The decontamination procedure of the microwave tubes was based on the method by BERGHOF (Cleaning Vessel Conditioning), using 10 ml of agua regia and parameters as shown in Table 7 in the microwave digester.

Table 7: Parameter settings of Speedwave®four by BERGHOF for the cleaning of the microwave tubes

Steps	Temperature	Time	Ramp	Power	Pressure
1	170 °C	5 min	5 min	90 %	50 bar
2	200 °C	15 min	1 min	90 %	50 bar
3	50 °C	15 min	1 min	0	0
4	50 °C	1 min	1 min	0	0
5	50 °C	1 min	1 min	0	0

3.3 Isotopic and Elemental Analysis by ICP-MS

Inductively Coupled Plasma Mass Spectrometry (ICP-MS) is an

instrumental analysis technique, which provides the determination of elements in a relatively short time. Because of its high detection capability, this technique is nowadays the most widely used technique for analysing ultra-trace elements. In addition to these characteristics, the technique can also be used for isotopic measurements with accuracies to 0.05 % in case of devices based on quadrupole type mass analysers (Skoog and Leary, 2009; Taylor, 2001; Thomas, 2004).

The components of ICP-MS are highlighted by the sample introduction system, usually using a nebulizer, the ionization source in form of the inductively coupled plasma, the mass analyser (quadrupole) and the ion detection system (Becker and Dietze, 1998).

The technique is based on the fact that each element has at least one isotope, whose ratio between the mass and the charge thereof is exclusive. The chemical compounds contained in the solution are decomposed into their atomic constitution by inductively coupled plasma and ionized with a high degree of ionization (90 % for majority of the elements), forming a fraction of ions of very small multiple loads (< 1 %). The mass analyser separates the ions by their mass/charge ratios, which are then detected by an electron multiplier. However, a factor that may significantly affect the analysis by ICP-MS is the occurrence of interference from various sources, which can affect the accuracy and the detection limits. These interferences are commonly classified to their origin, in spectral and non-spectral interferences (Becker and Dietze, 1998).

The elemental and isotopic analysis of the digested samples were performed by ICP-MS of the type X Series II (Thermo Fisher Scientific Inc.) using the instrumental and data acquisition parameters as shown in Table 8 and 9. The produced lead standard solutions had a concentration of 0 ng mL^{-1}, 0.5 ng mL^{-1}, 2.5 ng mL^{-1} and 5 ng mL^{-1}. Lead concentration was calculated by adding up the measured counts per second of the Pb isotopes (206; 207; 208) per sample and inserting them in the generated linear function of the concentration of the standard solutions.

Table 8: ICP-MS instrumental parameters

Nebulizer		Mira Mist
RF Power [W]		1450
Flow rate nebulizer gas [l min^{-1}]		0.8
Flow rate coolant gas [l min^{-1}]		13
Flow rate auxiliary gas [l min^{-1}]		0.7
Peristaltic pump rotation [RPM]		15
Torch	Sample depth [mm]	150
	Vertical [mm]	93
	Horizontal [mm]	53

Table 9: Data acquisition parameters

Measuring mode	Peak jump
Points per mass	3
Dwell time	4 ns for 206 and 207 Pb; 2 ns for 208
Sweeps	20450
Acquisition time per main run	300 s
Replicates	3

In one analysation campaign, always 8 sample filters were digested and their respective sample solutions analysed along with two filter blanks and two acid blanks.

For the determination of the isotopic ratios of Pb, equipment optimization tests in case of acquisition time, dead time and mass discrimination had to be performed before the analysis of lead isotope ratios in the samples could have been realized.

3.4 Statistical Analysis

Results were summarized into a multielemental database using Microsoft Excel 2016 and statistically characterized and analysed with the BioEstat 5.3 and ORIGIN 8 statistical softwares. As the data was not normally distributed, the nonparametric Kruskal–Wallis test was employed to investigate the

differences in lead concentrations and isotope ratios. The Kruskal-Wallis test statistic, H, was calculated as equation 1:

$$H = \frac{12}{N(N+1)} \sum_{i=1}^{k} \frac{{R_i}^2}{n_i} - 3(N+1) \qquad (1)$$

where n_i is the number of observations in group i, N the total number of observations in all k groups), and R_i the sum of the ranks of the n_i observations in group i.

To estimate which groups are differing significantly from each other, a Post-hoc test has to be performed. If the test results in a P-value of $P<0.05$, the resumption that the two groups are statistically equal to each other, has to be rejected (Zar, 1999).

3.5 Back Trajectory Calculation

In order to investigate the sources of lead in the particulate matter samples, air mass backward trajectories were calculated using the HYSPLIT model (Hybrid Single-Particle Lagrangian Integrated Trajectory, Version 4.7), a comprehensive modelling system provided by the National Oceanic and Atmospheric Administration (NOAA) Air Resource Laboratory (Draxler and Rolph, 2003). For detailed episode studies, trajectories ended at different height levels, i.e. 0 m; 100 m; 250 m AGL (above ground level), at 0900 UTC (1000 UTC for samples taken in daylight saving time period) representing 12:00 local time, arriving at the sampling point at the end of each sampling period. Run time of each back trajectory was 24 h or rather 48 h depending on the sampling time of each sampling period.

4 Study Locations

4.1 Study Location of Goiânia

The city of Goiânia, the capital of the Brazilian state of Goiás, is located in the Mid-West of Brazil and possessed 1.43 mi. inhabitants in 2015, owing a fleet of 1.103 mi. vehicles, which is a proportion comparable to highly

industrialized countries (IBGE, 2015). The city of Goiânia is located in the central region of Goiás, the sampling point is placed in the central area of the city along the old railway station under the following geographical coordinates: 16°66'31.86''S; 49°26'15.75''W (Figure 3). Sampling equipment was donated by SEMARH (Secretaria do Meio Ambiente e dos Recursos Hídricos). The location of the sampling point has a strategic importance. The surrounding area is densely occupied by public buildings (town hall of Goiânia, Court of Auditors of the Municipality, main bus station and hospitals), private buildings intended for trade in general (Goiânia Station, Araguaia Shopping, supermarket and hotels) and periodically the largest street market in the city of Goiânia, which attracts thousands of people from the city and the region. The near Praça da Estação is lined by avenues and streets with a high traffic flow (Avenida Goiás Norte, Avenida Independência and Rua 44).

Figure 3: Location of the sampling point in Goiania (Source: COSTA e SILVA, 2015)

4.1.1 Climate of Goiânia

The climate in the municipality of Goiânia according to the Köppen climate classification is type *Aw*, tropical humid with two distinct seasons, an almost cold and dry winter from May to October and hot and rainy summer from November to April. In the hottest months, the maximum temperatures vary

between 29 °C and 35 °C, while in the coldest months of the year, the minimum temperatures can reach 13 °C (Alvares et al., 2005).

The summers are characterized by rapid changes in daily weather conditions, with rains of short duration and high intensity, accompanied by thunderstorms and high wind gusts. But also short dry seasons with periods of drought lasting 7 to 15 days can occur in this time of the year. The amount of precipitation can oscillate between 1,200 and 2,500 mm between the months of September to April. In the fall, temperatures become milder due to the entry of cold air masses with minor temperatures between 12 ºC and 18 ºC and average maximums of 28 ºC. The relative humidity is high with values reaching up to 98 %. The winter brings the typically dry climate of the Cerrado biome, with low moisture content, reaching extreme low humidity values. In September, with the beginning of spring, the rains become more intense and frequent again (Governo Goiás, 2016).

4.1.2 Geology of Goiânia

Goiânia is located on the Brasília Fold Belt, which is situated between the Craton of São Francisco and the Massive of Goiás. This fold-and-thrust-belt is formed by a greenstone belt and high metamorphic rocks (Fonseca et al., 1995; Ulhein et al., 2012; Pimentel and Fuck, 1992).

Granite-greenstone terrains occupy a substantial part of Goiás, including large tracts of granitic-gneissic rocks of a granodioritic to tonalitic composition, metamorphosed in the green schist facies to amphibolite, generally mylonitized and ultramylonitized (Danni et al., 1982). The Annapolis-Itauçu granulitic complex, located in the north-west and the center of the Folha Goiânia, is formed by basic to ultrabasic and metasedimentary components, represented by impure quartzites, calcisilicatic rocks, impure marbles and aluminous to hyper-aluminous gneisses. This granolithic complex is genetically related with the Orthogneissic-Migmatic Formation (Associação Ortognáissica-Migmatítica), which forms a belt from the north of the Folha Goiânia to its south-east, where calcium-sodic, tonalitic and granodioritic orthogneisses are dominating. The metasediments of the Faixa Uruaçu range, distributed in the south-west and

north-east edges of the Folha Goiânia, are defined as Middle Proterozoic, present as a recumbent fold structure with metamorphism of the "Barrowianan" type, showing an increasing intensity from east to west (Fuck and Marini, 1981).

4.1.3 Pedology of Goiânia

In Goiania, as in the biggest part of the state of Goiás, latosols with a low till medium fertility are the predominant soils, especially in form of dystrophic dark yellow latosol and alic red-yellow latosol. In this soils, clays of the kaolinite type are typical, whose particles are coated with iron oxides, which are responsible for the typical reddish colours. The transition between the soil horizons is gradual or diffuse, except the darkening in the A horizon. The B horizon structure is composed of rounded and very small (0.5 to 3.0 mm) aggregates, leaving a lot macro pores between them, which provides a high water permeability even with high levels of clay (Silva and de Castro, 2002).

Another soil type in this region is the alic yellow-red podsol. These soils have a sub superficial horizon of accumulated clay, as clay particles migrate from the A horizon and deposit in the B horizon. Thus, the most superficial layers (horizons A and E) are sandier. Compared to latosols, yellow-red podsol shows a less shallower, slightly larger proportions of silt, minerals with little resistant to weathering and a remarkable differentiation of their horizons (Silva and de Castro, 2002).

4.2 Study Location of Rio Claro

The city of Rio Claro, owing 199.961 inhabitants (IBGE, 2015), is located in the middle east of the Brazilian state of São Paulo, belonging to the large ceramic center of Santa Gertrudes, which also includes the cities of Limeira, Ipeuna, Cordeirópolis, Araras and Piracicaba, integrated in the association of ASPACER (Associação Paulista das Cerâmicas de Revestimento). The production of ceramic in this region reached 760 million m² in 2010, representing 83% of the total production in São Paulo and 56 % in Brazil, considered as the biggest ceramic production centre in Latin America and the

second biggest in the world. Besides ceramic production, the region faces environmental problems derived from the burning of sugar cane plantations, mainly in the dry season, when the air quality decreases drastically (ASPACER, 2011).

The particulate matter sampling point was installed at the Campus Bela Vista, near CEAPLA, at the terrain of the Instituto de Geociências e Ciências Exatas (IGCE) of the State University of São Paulo (UNESP) in Rio Claro (Figure 4), located at the geographic coordinates with a latitude of 22º39' 22.30''S, a longitude of 47º54' 59.11''W and an altitude of 626.5 m.

Figure 4: Location of the sampling point in Rio Claro (Source: Lorenzeto de Abreu, 2014)

4.2.1 Climate of Rio Claro

The climate classification system of Köppen ranks the region of Rio Claro as *Cwa* (temperate with cold winters). The region is subjected to two distinct seasons, dry season from April to September and rainy season from October to March. Dry season shows an average temperature of 17 °C, while in rainy season average temperature is above 22 °C (Troppmair, 1992). Annual rainfall is above 1500 mm, of which 77 % are concentrated in the rainiest months (October to March) (Alvares et al., 2005). Considering the year 2005, the maximum precipitation occurred in January (482.2 mm) and the minimum in

July (3.6 mm), the total annual precipitation amounted 1398.3 mm (Estação Meteorológica de Rio Claro (CEAPLA), 2005).

The prevailing winds of the region of Rio Claro come from the south and south-east, justifying the location of the industrial district in the northern part of the city in order to avoid air pollution (Troppmair, 1992).

4.2.2 Geology of Rio Claro

Rio Claro is located in the center of the Corumbataí river basin, situated in the north-east part of the Paraná Sedimentary Basin, which belongs to the Peripheral Paulista Depression in the middle-east of the state of São Paulo. This depression belongs to the outcrop area of Palaeozoic (Itararé group, Tatuí formation and Passa Dois group – Irati and Corumbataí formation), Mesozoic (Pirambóia formation, São Bento group – Botucatu and Serra Geral formation, intrusive magmatic rocks – dykes and sills, and Itaqueri formation) and Cenozoic (Rio Claro formation) rocks (Almeida, 1964; Melo, 1995).

The Corumbataí river flows from its source in the region of Analândia, to its mouth, the Piracicaba river, along on various rock types as mentioned with the stratigraphic units above. Due to the structure caused by the Pitanga Dome, the stratigraphic units of the upper river course (Botucatu, Pirambóia and Corumbataí formation) and the lower river course (Corumbataí formation) are younger than the average course (Itararé Group and Tatuí formation). The Pitanga Dome is a Mesozoical structural high, today topographically downgraded by the drainage of the Corumbataí river basin, which promotes the appearance of Paleozoic rocks from the base of the stratigraphic column of the Paraná Sedimentary Basin in this region (Almeida, 1964; Penteado, 1976).

4.2.3 Pedology of Rio Claro

In the city of Rio Claro, sandstone rocks and consequently sandy soils are predominant. This soils have a fast rainwater infiltration and a high percolation to the horizon. Thus, leaching is dominant in the soil horizons, turning the soils acid and poor in nutrients. These soils are predominantly

occupied by grasslands and the forestation of eucalyptus (Troppmair, 1992). In Rio Claro occur basically three types of sandy soils. The yellow-red podsol with a medium-clayey texture is present at low topographies like in the valleys of Corumbataí River and Ribeirão Claro. This soil is formed from fine sediments of the Passa Dois and Tubarão group (Cottas, 1983). Red-yellow latosols are also present in this region as well as purple latosols, which have a clayey to very clayey texture. Another type of soil of this region, but present in little distribution, are the lithic soils, whose main feature is its small profoundness (less than 30 cm). These soils are associated with siltstones and argillites from the Corumbataí formation and with diabase intrusions from the Serra Geral. Furthermore, hydromorphic soils occur related to alluvial sediments in the area, restricted to the valleys of Corumbataí River and Ribeirão Claro (Cottas, 1983; Oliveira et al., 1999).

5 Results and discussions

5.1 Preliminary Studies

5.1.1 Acquisition Time Optimization

To obtain the optimal acquisition time for the subsequent analysis of the particulate matter samples, an experiment was conducted, where lead standards with different concentrations (0.25 ng mL^{-1}, 0.75 ng mL^{-1}, 1 ng mL^{-1}) were analysed by ICP-MS for their $^{206}Pb/^{207}Pb$ and $^{208}Pb/^{207}Pb$ ratios at two different acquisition times (5 min and 10 min) in five main runs. Subsequently, the precision in form of the relative standard deviations (RSD) of the five main runs for each obtained ratio was compared to the appropriate theoretical values, which were calculated by the following equation:

$$\mathrm{RSD} = \sqrt{\frac{1}{c_1} + \frac{1}{c_2}} \times 100 \qquad (2)$$

where c_1 is the measured incoming counts per second for the first isotope and c_2 is the measured incoming counts per second for the second isotope obtained

by ICP-MS.

As expected, for the calculated Pb isotope ratios, the relative standard deviations obtained by an acquisition time of 10 min were always lower than the standard deviations of the same samples at 5 min of acquisition time. In contrast to this, the experimental obtained values differ highly from the theoretical standard deviations, as in four cases the relative standard deviations of 5 mins of acquisition time showed a lower value then the values of 10 min of acquisition times for the same sample (Figure 5). This results emphasize that an application of a high acquisition time of 10 min for the further isotopic determination of the particulate matter samples is unessential with regard to the precision and also to the saving of time and costs. Thus, an acquisition time of 5 mins was applicated for the further isotopic analysis of the particulate matter samples.

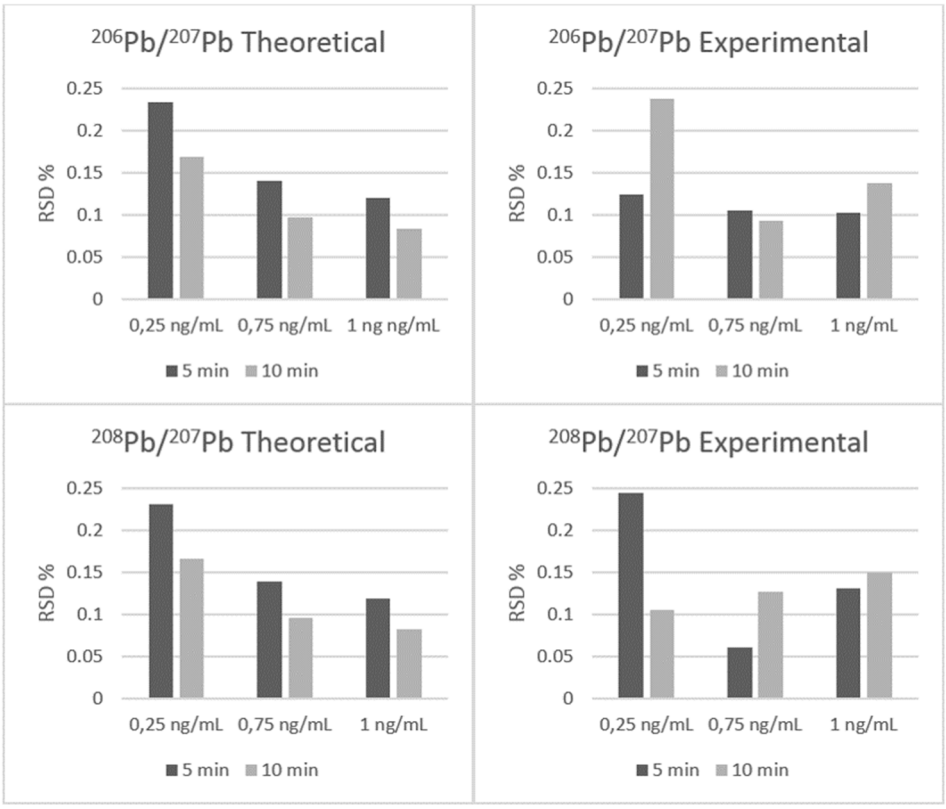

Figure 5: Theoretically calculated and experimentally obtained relative standard deviations of $^{206}Pb/^{207}Pb$ and $^{208}Pb/^{207}Pb$ isotope ratios for different concentrations at 5 min and 10 min of acquisition time

5.1.2 Dead Time Determination

An accurate determination of the detector dead time is indispensable, if accurate isotope ratio measurements with ICP-MS are to be made. Detector dead time is considered as the time for which the ion counting system is unable to record incoming ions after the impact and detection of a previous ion (Knoll, 2000). This results in counting losses increase in magnitude as the counting rate increases. Because of this fact, inconsistencies in isotope abundance ratio measurements occur, which are independent of mass discrimination effects and on account of this, has to be accurately corrected prior to correcting mass discrimination. The dead time is a feature of the ion counting electronics and the detector itself. (Jarvis, 1992).

In order to find the optimal dead time adjustment for the analysis of the particulate matter samples by ICP-MS, four lead standard solutions with different concentrations (2 ng mL^{-1}, 4 ng mL^{-1}, 8 ng mL^{-1}, 10 ng mL^{-1}), produced from NIST Standard Reference Material 981, were prepared and analysed by ICP-MS on their $^{208}Pb/^{207}Pb$ ratios at different dead time adjustments (20 ns, 30 ns, 40 ns, 50 ns and 60 ns).

The measured $^{208}Pb/^{207}Pb$ isotope ratios for each standard concentration were normalised (=($^{208}Pb/^{207}Pb$)measured/true value) and recorded in a diagram with the $^{208}Pb/^{207}Pb$ ratios plotted against the detector dead time (Figure 6). The polynomial trendlines of the $^{208}Pb/^{207}Pb$ ratios for each concentration were added to the diagram for obtaining the optimal dead time of the detector, which is shown by the point of intersection of the lines. In this case, the dead time of the detection system was observed as 34 ns. This value was adopted to the parameter settings of the ICP-MS and applicated for the further elemental and isotopic determination of the particulate matter samples.

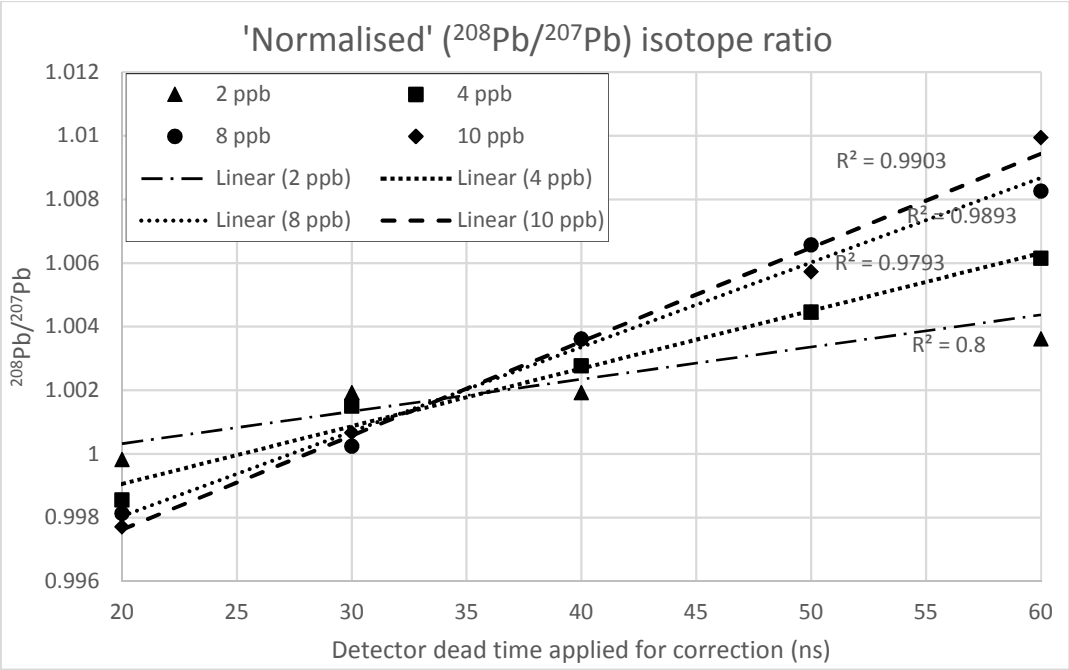

Figure 6: Normalized $^{208}Pb/^{207}Pb$ isotope ratio plotted as a function of the value applied for dead time correction of the 'raw' results obtained for solutions with a Pb concentration ranging from 2 to 10 ppb

5.1.3 Mass Bias Correction

The differential transmission of ions of different masses from the point at where the ions enter the sampling device until they finally are detected by the electron multiplier is called mass bias effect. This effects occur principally in the interface region of the magnetic sector of the ICP. It is considered, that several processes conduce to this effect, *e.g.* the space charge effect in the plasma or vacuum interface regions (Jarvis, 1992).

The mass bias was corrected by measuring an isotopic standard of Pb (2.5 ng mL^{-1}) and calculating a correction factor by using the following mathematical expression:

$$\frac{R_{true}}{R_{obs}} = (1 + \varepsilon linear.\Delta m) \qquad (3)$$

where R_{true} is the corrected isotope ratio; R_{obs} is the experimental obtained isotope ratio; Δm is the difference of the atomic weights between the two isotopes and $\varepsilon linear$ is the correction factor.

5.2 Results and Discussion for Studies in Goiânia

5.2.1 Elemental Determination of Lead in Samples from Goiânia

Figure 7 demonstrates one of the analytical curves of the standard solutions used for the quantification of lead in Goiânia, showing a coefficient of correlation of $R^2 = 0.9999$, which represents a very high linear relationship. All analytical curves of the used standard solutions had coefficients of determination values of at least $R^2 = 0.9995$.

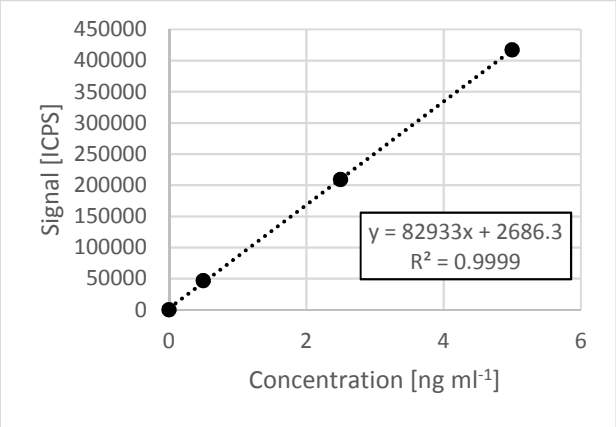

Figure 7: Analytical curve for the quantification of Pb via ICP-MS

Figures 8 (April/May) and 9 (August) represent the obtained lead concentrations from Goiânia in ng mL^{-1} in the sample dilutions along with the lead concentrations in the respective filter blank dilutions and acid blanks. The standard deviation of the lead concentrations of the three main runs is amounted for each sample or blank on the respective bar in the diagram. Instrumental detection limit, which is equal to three times the standard deviation of the blank signal at the selected analytical masses, was identified as 0.0035 ng mL^{-1}. The method detection limit had a value of 0.014 ng mL^{-1}.

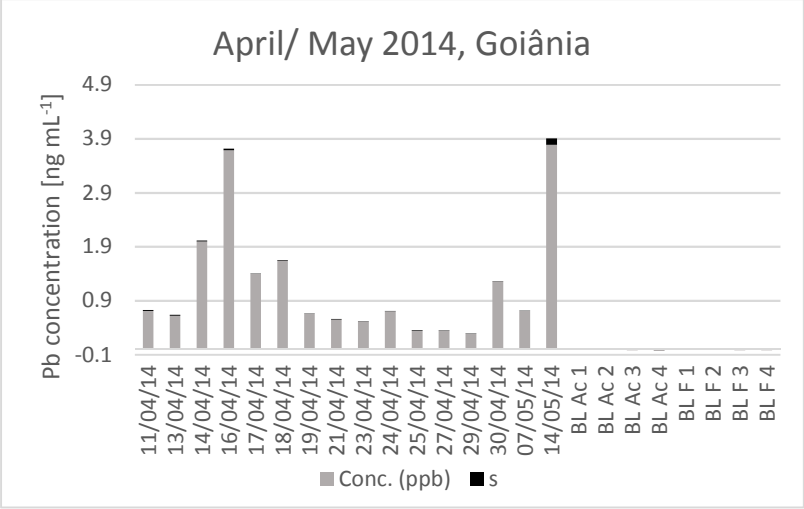

Figure 8: Pb concentrations (Conc.) and respective standard deviations (s) in ng ml^{-1} in sample and blank dilutions of Goiânia samples from April and May 2014 (BL Ac = Acid blank, BL F = Filter blank)

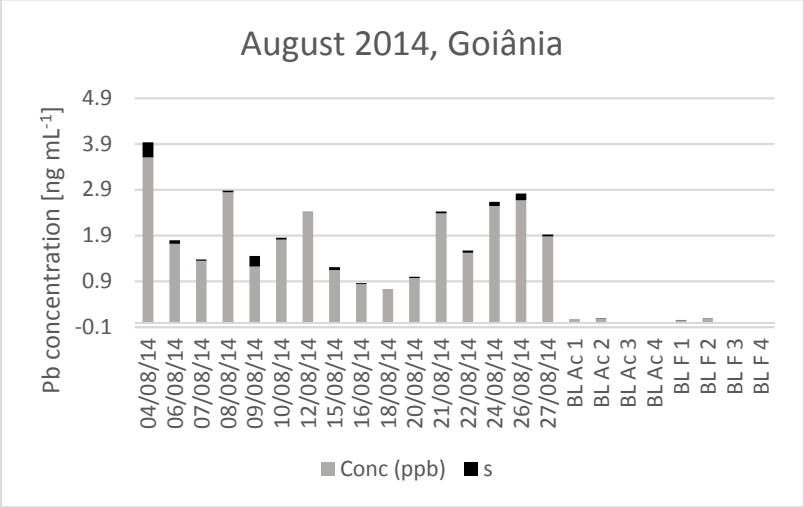

Figure 9: Pb concentrations (Conc.) and respective standard deviations (s) in ng ml^{-1} in sample and blank dilutions of Goiânia samples from August 2014 (BL Ac = Acid blank, BL F= Filter Blank)

In order to receive the lead concentration per volume of air, the determined volume of the Pb concentration in the sample solutions in ng mL^{-1} were calculated to the mass of Pb per m^3 of air by multiplicating the Pb concentration in the sample dilution with the final volume of the solution and dividing it through the respective sampled volume of air. The results are presented in the Figures 10 and 11.

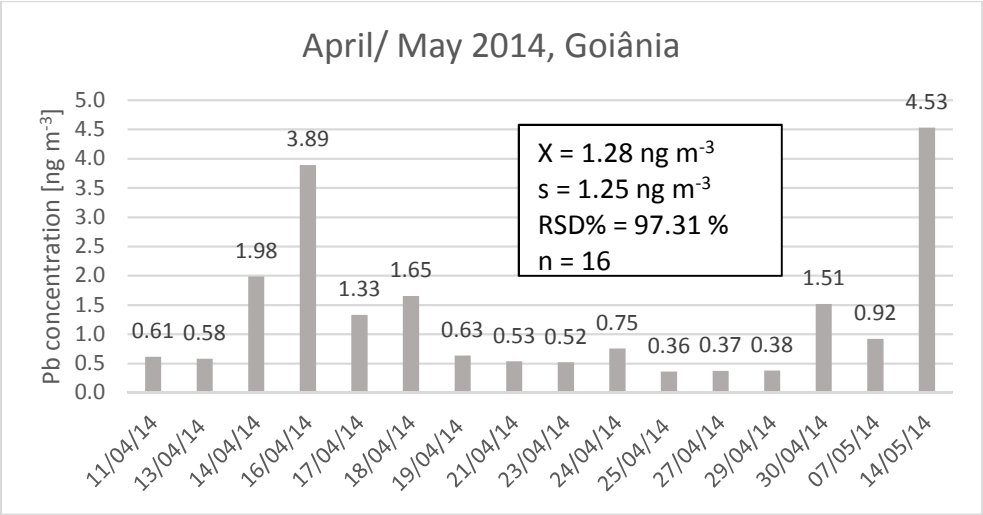

Figure 10: Pb concentration in ng m^{-3} for Goiânia samples from April and May 2014 (X = mean value; s = standard deviation; RSD% = relative standard deviation; n = quantity)

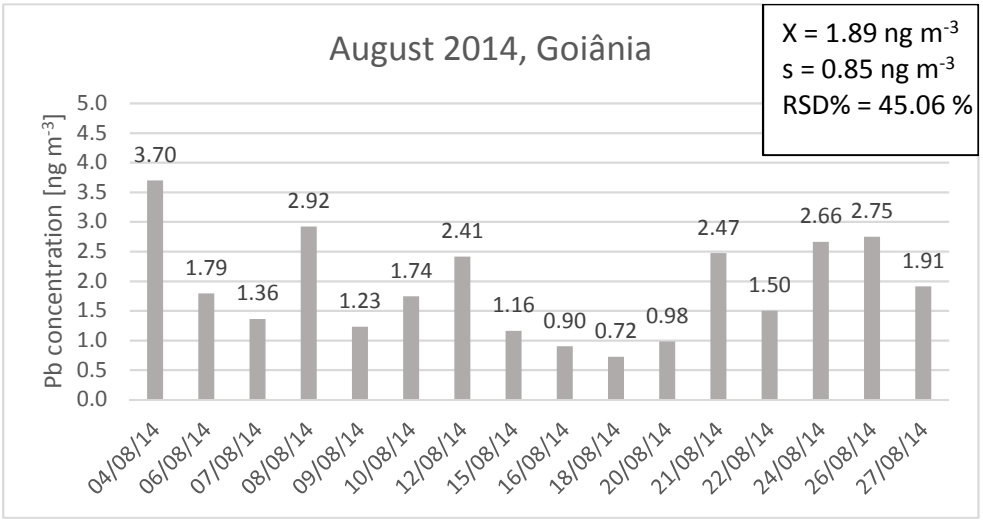

Figure 11: Pb concentration in ng m^{-3} for Goiânia samples from August 2014 (X = mean value; s = standard deviation; RSD% = relative standard deviation; n = quantity)

The Pb concentrations of the Goiânia samples show a high disparity between rainy season samples (April/May) and dry season samples (August). The average Pb concentration from April is lower with a mean value of 1.28 ng m^{-3} than the mean Pb concentration from August with 1.89 ng m^{-3}. Furthermore, samples of rainy season show a considerably higher coefficient of variation with 97.31 % compared to 45.06 % of the samples from dry season, demonstrating a high divergence within the rainy season samples. Samples from April/May differ from 0.36 ng m^{-3} to 4.53 ng m^{-3}. Two samples have a higher concentration than 3 ng m^{-3}, no other sample of this campaign shows a higher value than 2 ng m^{-3}. This outlier values may could be attributed to a possible sample contamination.

In contrast, August samples differ from 0.72 ng m^{-3} till 3.70 ng m^{-3}. Six samples from August have a higher Pb concentration than 2 ng m^{-3}, one sample show a higher concentration than 3 ng m^{-3}. Median and arithmetic average of the rainy season samples differ considerably while median and arithmetic average of dry season samples are quite close to each other (Table 10). The high variation of April samples is also expressed in the asymmetry, where this samples show a value of 1.871, whereas August shows a value closer to 0 with 0.532.

Table 10: Descriptive statistics of rainy season (April 2014) and dry season (August 2014) samples from Goiânia

	Rainy Season 2014	Dry Season 2014
Sample size	16	16
Minimum	0.360	0.720
Maximum	4.530	3.700
Total Amplitude	4.170	2.980
Median	0.690	1.765
First Quartile (25%)	0.528	1.213
Third Quartile (75%)	1.545	2.518
Interquartile Deviation	1.018	1.305
Arithmetic Average	1.284	1.888
Variance	1.564	0.726
Standard Deviation	1.250	0.852
Standard Error	0.313	0.213
Coefficient of Variation	97.40%	45.14%
Asymmetry	1.871	0.532

Also, both sample periods show differences in their quartiles as shown in the generated boxplot diagram (Fig. 12). While 25 % of April samples are lower than 0.528 ng m^{-3}, just 25 % of August samples are lower than 1.765 ng m^{-3}. Even with the two high outlier values, just 25 % of the April samples show higher Pb concentrations than 1.545 ng m^{-3}, while 25 % of the August samples reach higher Pb concentrations than 2.518 ng m^{-3}. Due to the two outlier values, arithmetic average of rainy season samples is stretched to a higher value. This data demonstrates that in general dry season samples show markedly higher Pb concentrations and differ in a much lower scope than samples from rainy season.

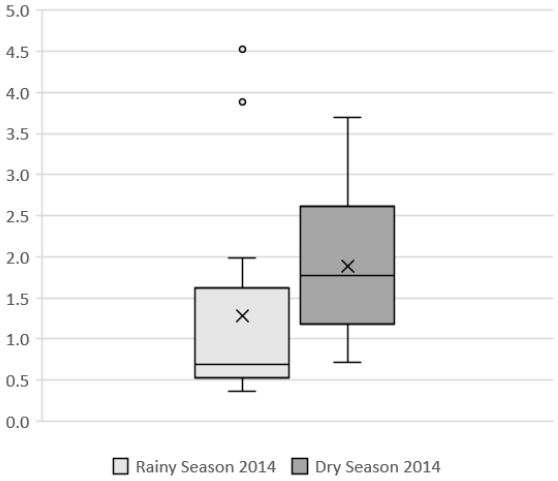

Figure 12: Boxplot diagram for Pb concentrations of samples from rainy and dry season 2014 from Goiânia

To further examine differences in the Pb concentrations between the two sample periods, a Kruskal-Wallis test was performed. The result of the test demonstrated a H-value of 5.8182 and P-value lower than 0.05 (P= 0.0143), rejecting the H_0 hypothesis that both sample groups are equal and showing that Pb concentrations from April and August are statistically different to each other.

No lead concentration value exceeded the guide values established by CETESB, the European Union or United States Environmental Protection Agency. In comparison with a previous study by Bollhöfer and Rosman (2000), where Pb concentration in particulate matter from São Paulo City ranged between 3 ± 1 and 52 ± 14 ng m^{-3} with an average of 29 ng m^{-3}, Pb concentrations from Goiania are relatively low. Also, the study from AILY (2001) shows clearly higher Pb concentrations ranging from 10.23 ng m^{-3} to even 254.52 ng m^{-3} in particulate matter sampled in São Paulo City. In that study, dry season samples with an average value of 60.56 ± 43.38 ng m^{-3} showed higher Pb concentrations than in rainy season with an average of 36.14 ± 37.80 ng m^{-3}.

5.2.2 Back Trajectory Analysis of Sampling Point in Goiânia

Back trajectories with a run time of 24 hours were calculated for sampling dates in rainy and dry season with markedly elevated (higher than or near 75 % quartile) and low concentration levels (lower than or near 25 % quartile) of lead

in order to assess directions of air masses and hence possible sources of Pb in Goiânia samples. Trajectory plots ended respectively at the end of each sampling date at three different heights (0 m, 100 m, 250 m AGL).

In rainy season at sampling dates with elevated Pb concentrations (14th, 16th, 18th April, 14th May) all air masses came from eastern direction, originated in the hilly landscape in the north of the state of Minas Gerais, passing the Serra dos Christais and the eastern suburbans of Goiânia, mainly through low heights up to 500 m AGL (Fig. 13).

At sampling days in rainy season with low Pb concentrations (11th, 21th, 23th and 29th April), direction of air masses varied between east, north-east, and south-east direction (Fig. 14). Air masses from eastern direction showed similar trajectories as at sampling days with high Pb concentration, but passing greater heights up to 800 m AGL. Trajectories from north-eastern direction originated in the mountain ridges of the Serra Geral do Parana and moved across the city of Brasilia to Goiânia, while air masses from south-eastern direction passed from the hills of Serra do Conforte to Goiânia in heights up to 500 m AGL.

In dry season for sampling days with high Pb concentrations (4th, 8th, 21th and 26th August), no pattern of direction is distinguishable (Fig. 15). Air masses coming from southern and south-eastern direction from the elevated plains, passing low heights between 50 and 250 m AGL, and from eastern direction, where trajectories travelled in great heights up to 1400 m AGL from the Serra dos Christais westward to Goiânia.

On sampling days with low Pb concentrations in dry season (7th, 9th, 18th and 20th August), a pattern that all trajectory plots came from east direction is recognizable. While trajectories originated in low heights in the north of Minas Gerais, they increased their height up to 500 m before arriving in Goiânia (Fig. 16).

Hence, back trajectory analysis shows that on days with elevated lead concentrations in rainy season, air masses came from eastern direction and heights up to 500 m, while on days with low Pb concentration no trend was recognizable. In contrast to that, in dry season on days with high Pb concentration, no pattern of air mass direction was estimated, whereas on days with lower Pb concentrations air mass directions showed the trend to come from

eastern direction, travelling in heights up to 500 m.

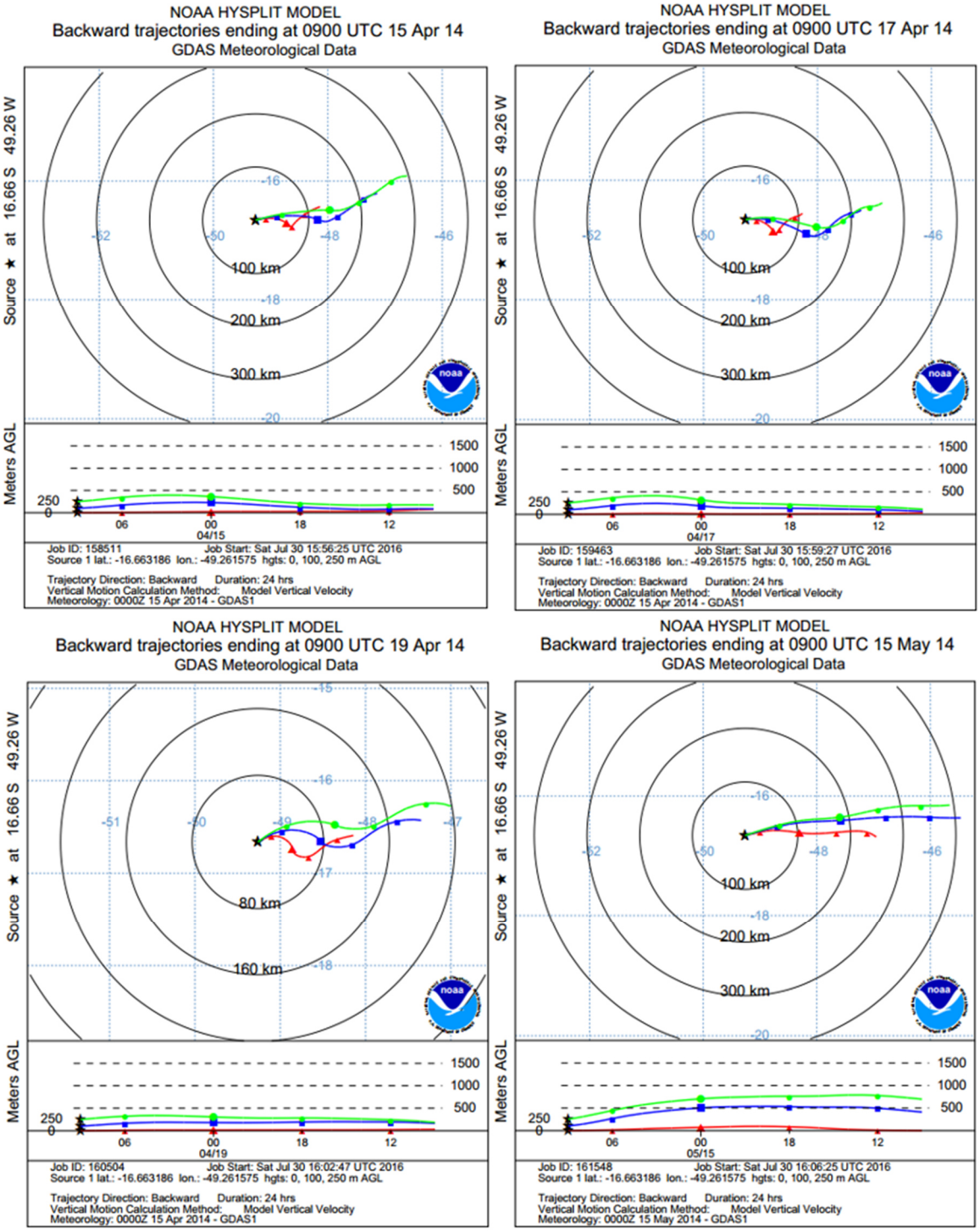

Figure 13: Back trajectory plots ending at three different height levels (0 m; 100 m; 250 m AGL) on episodic dates with elevated Pb concentrations in rainy season arriving at sampling point in Goiânia

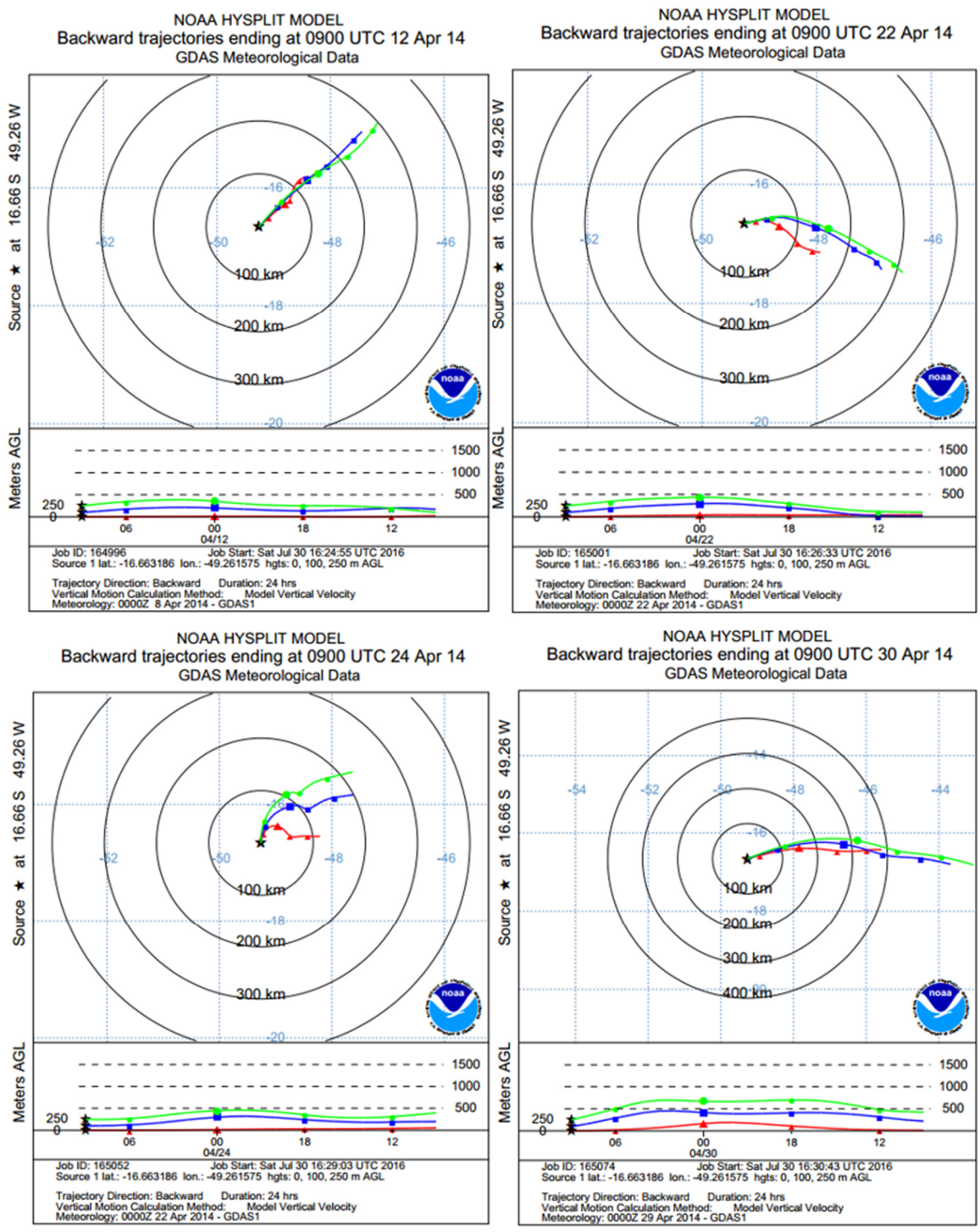

Figure 14: Back trajectory plots ending at three different height levels (0 m; 100 m; 250 m AGL) on episodic dates with low Pb concentrations in rainy season arriving at sampling point in Goiânia

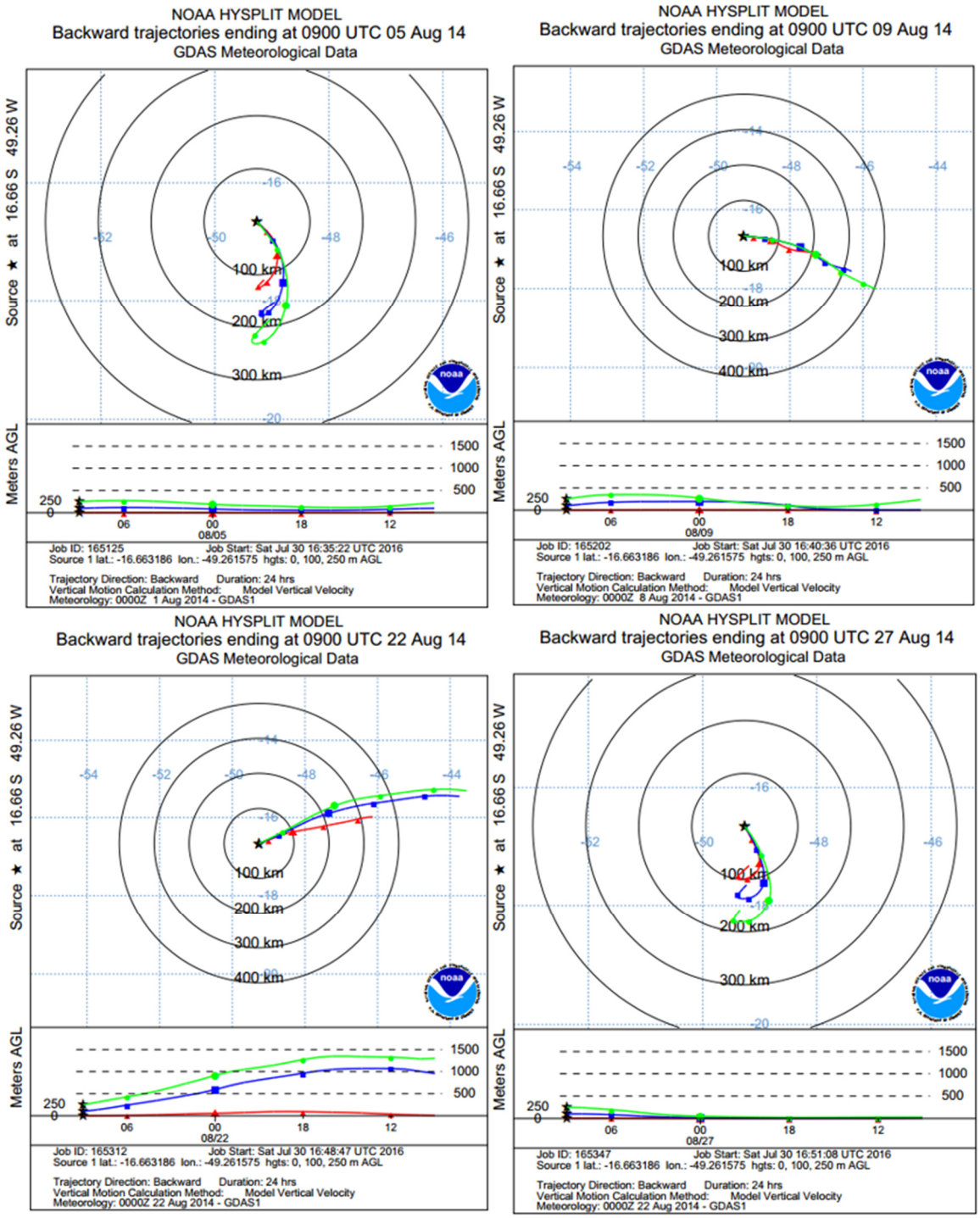

Figure 15: Back trajectory plots ending at three different height levels (0 m; 100 m; 250 m AGL) on episodic dates with elevated Pb concentrations in dry season arriving at sampling point in Goiânia

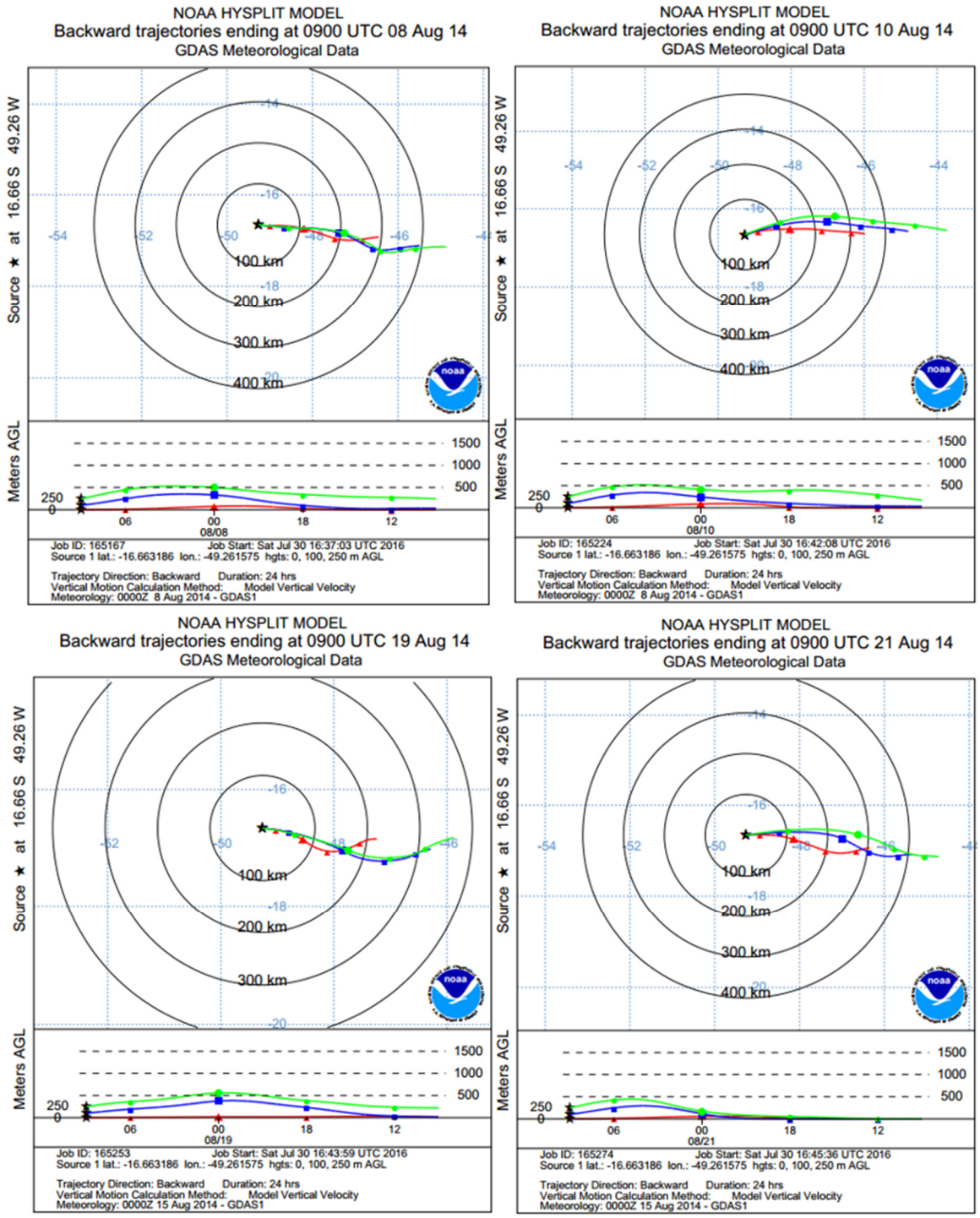

Figure 16: Back trajectory plots ending at three different height levels (0 m; 100 m; 250 m AGL) on episodic dates with low Pb concentrations in dry season arriving at sampling point in Goiânia

5.2.3 Isotopic Determination of Lead in Samples from Goiânia

The tables 11 and 12 show the mass bias corrected $^{206}Pb/^{207}Pb$ and $^{208}Pb/^{207}Pb$ isotope ratios with the afore mentioned equation (2) along with their relative standard deviations (RSD) for three main analysing runs. For an accurate lead isotope evaluation, it is intended to have a RSD of <0.2 % for the isotope ratios.

Table 11: Corrected lead isotope ratios of Goiânia samples from rainy season (April/May 2014) with their relative standard deviations (X = mean value; s = standard deviation; RSD% = relative standard deviation)

Date	$^{206}Pb/^{207}Pb$	RSD%	$^{208}Pb/^{207}Pb$	RSD%
11/04/14	1.1711	0.077	2.4495	0.162
13/04/14	1.1757	0.112	2.4462	0.111
14/04/14	1.1731	0.048	2.4465	0.158
16/04/14	1.1751	0.038	2.4505	0.030
17/04/14	1.1737	0.040	2.4522	0.089
18/04/14	1.1721	0.210	2.4475	0.081
19/04/14	1.1737	0.093	2.4512	0.075
21/04/14	1.1620	0.190	2.4406	0.304
23/04/14	1.1717	0.247	2.4492	0.117
24/04/14	1.1660	0.240	2.4436	0.264
25/04/14	1.1727	0.379	2.4512	0.190
27/04/14	1.1761	0.212	2.4495	0.106
29/04/14	1.1757	0.246	2.4482	0.117
30/04/14	1.1711	0.026	2.4505	0.135
07/05/14	1.1667	0.173	2.4452	0.107
14/05/14	1.1717	0.191	2.4442	0.147
X	1.1718	0.158	2.4479	0.137
s	0.0039		0.0033	
RSD%	0.3323		0.1331	

Table 12: Corrected lead isotope ratios of Goiânia samples from dry season (August 2014) with their relative standard deviations (X = mean value; s = standard deviation; RSD% = relative standard deviation)

Date	$^{206}Pb/^{207}Pb$	RSD%	$^{208}Pb/^{207}Pb$	RSD%
04/08/14	1.1608	0.243	2.4370	0.182
06/08/14	1.1839	0.054	2.4460	0.008
07/08/14	1.1689	0.078	2.4380	0.040
08/08/14	1.1688	0.075	2.4401	0.034
09/08/14	1.1749	0.080	2.4459	0.107
10/08/14	1.1779	0.044	2.4520	0.075
12/08/14	1.1729	0.117	2.4499	0.092
15/08/14	1.1760	0.099	2.4459	0.073
16/08/14	1.1779	0.200	2.4480	0.169
18/08/14	1.1749	0.060	2.4499	0.063
20/08/14	1.1839	0.154	2.4490	0.127
21/08/14	1.1729	0.112	2.4489	0.071
22/08/14	1.1789	0.163	2.4510	0.153
24/08/14	1.1739	0.205	2.4460	0.079
26/08/14	1.1749	0.079	2.4459	0.108
27/08/14	1.1789	0.064	2.4460	0.108
X	1.1750	0.114	2.4462	0.093
s	0.0057		0.0044	
RSD%	0.4880		0.1808	

Measured $^{208}Pb/^{207}Pb$ isotope ratios from April/May samples show a good precision with just one RSD value higher than 0.2 %, while there are six RSD values higher than 0.2 % at the $^{206}Pb/^{207}Pb$ isotope ratios. In contrast, August samples show a higher precision with just three RSD values higher than 0.2 % at the $^{206}Pb/^{207}Pb$ isotope ratios and no RSD value higher than 0.2 % at $^{208}Pb/^{207}Pb$ isotope ratios. The higher precision in dry season samples is explicable with the higher Pb concentrations in this sampling period.

Pb–Pb diagrams were represented in previous studies with the aim of analysing, interpreting and comparing data. In this work, it has been used to plot the difference of $^{208}Pb/^{207}Pb$ and the $^{206}Pb/^{207}Pb$ ratios between both sampling periods (Fig. 17).

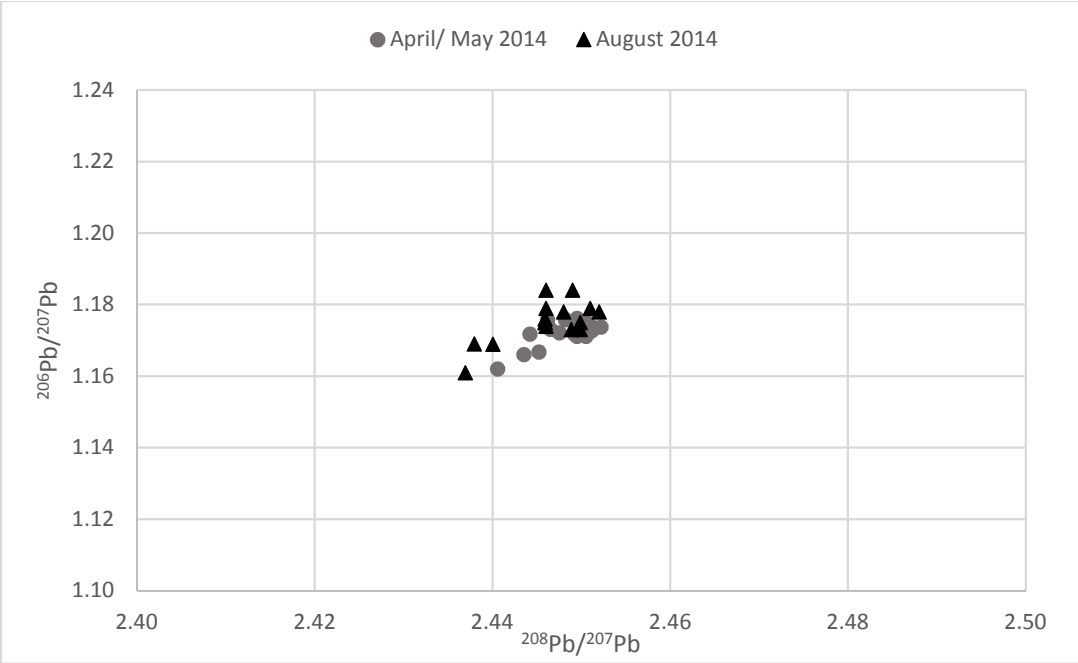

Figure 17: Pb–Pb diagram according to the Pb isotope ratios for samples taken in Goiânia

The $^{206}Pb/^{207}Pb$ isotope ratio varied in the rainy season samples from 1.1620 to 1.1761 and the variation of the $^{208}Pb/^{207}Pb$ isotope ratios accounted from 2.4460 to 2.4522. The $^{206}Pb/^{207}Pb$ isotope ratios from dry season samples differed from 1.1608 to 1.1839 and $^{208}Pb/^{207}Pb$ isotope ratios from 2.4370 to 2.4520. Arithmetic averages of $^{206}Pb/^{207}Pb$ isotope ratios of August samples are slightly higher (1.1750) than in April/May (average of 1.1718), while the $^{208}Pb/^{207}Pb$ ratios show just a marginally divergence (2.4462 in dry season and 2.4479 in rainy season). The relative standard deviations of all ratios demonstrate a higher variation of the $^{206}Pb/^{207}Pb$ isotope ratios in dry season than in rainy season, while the $^{208}Pb/^{207}Pb$ isotope ratios show very close relative standard deviations in both months. Kruskal-Wallis tests show, that $^{206}Pb/^{207}Pb$ isotope ratios from rainy season vary significantly from dry season (H= 4.3063, P= 0.0382), whereas $^{208}Pb/^{207}Pb$ isotope ratios between both sample periods show no significant statistical disparities (H= 1.3681, P= 0.2421). Thus, while $^{208}Pb/^{207}Pb$ isotope ratios in rainy and dry season demonstrate quite similar values, $^{206}Pb/^{207}Pb$ isotope ratios of dry season are in average higher than $^{206}Pb/^{207}Pb$ isotope ratios in rainy season. This observation supposes an enrichment of ^{206}Pb isotopes in dry season.

In order to assess possible emission sources, measured $^{208}Pb/^{207}Pb$ and

$^{206}Pb/^{207}Pb$ isotope ratios were plotted on a Pb-Pb diagram (Fig. 18) together with data from previous studies from Brazil, which contain Pb isotope ratios of aerosol samples from São Paulo (Bollhöfer and Rosman, 2000), gasoline, industrial emission and exhaust fume samples from São Paulo (Aily, 2001) and atmospheric deposit samples from Rio Grande (Mirlean et al., 2005).

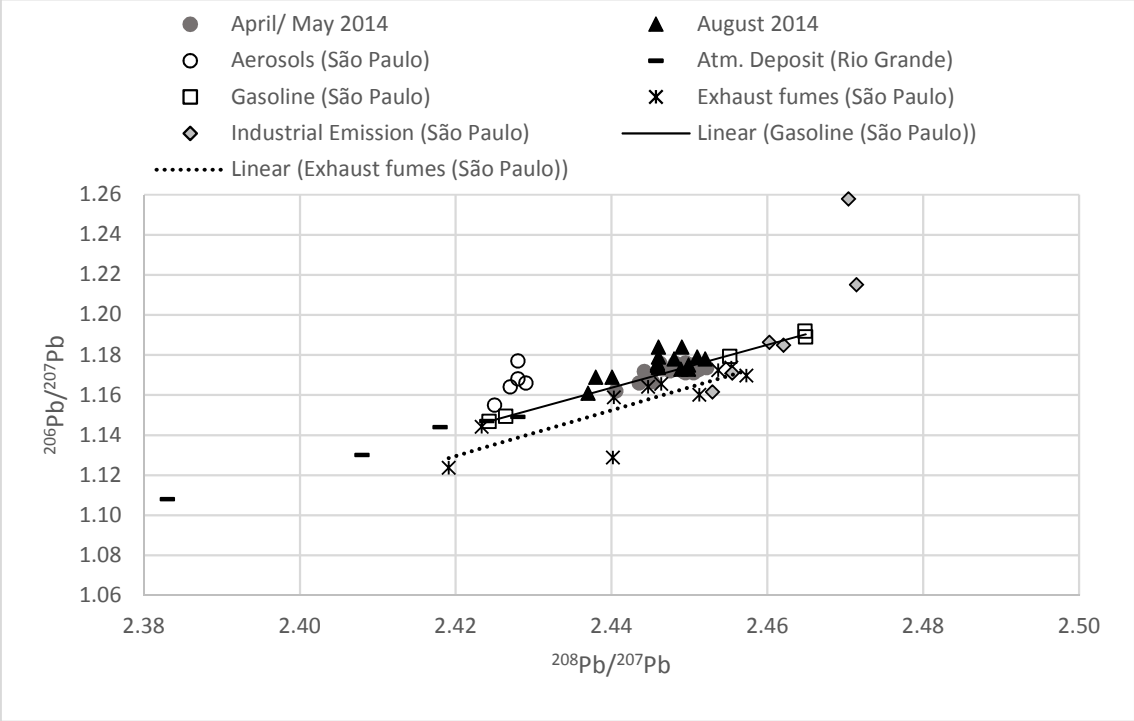

Figure 18: Pb–Pb diagram according to the Pb isotope ratios for samples taken in Goiânia compared with Pb isotope ratios from recent studies from Brazil

Pb isotope ratios in aerosol samples from São Paulo and atmospheric deposit samples from Rio Grande are highly different from Pb isotope ratios in Goiânia samples. Both, Pb isotope ratios from rainy season and dry season samples of Goiania, are slightly located on the line of gasoline Pb isotope ratios from São Paulo. Thus, gasoline can be considered as a possible influence on Pb isotope ratios of Goiânia, even though Pb isotope ratios from gasoline samples are distributed in a broader range with a low quantity of samples. Pb isotope ratio data of exhaust fumes from São Paulo is also distributed near isotope ratios from Goiânia samples, supporting the assumption that Pb isotope ratios of Goiânia may could be characterised by traffic emissions. Industrial emissions show a high variability grade in its isotope ratios, but also could be a factor of influence on Pb isotope ratios from Goiânia, especially for August

samples, which show higher $^{206}Pb/^{207}Pb$ isotope ratios and thus, are closer located to the Pb isotope data of industrial emissions.

In order to investigate contribution from the decay of Thorium to the Pb in PM in Goiânia, ratios of $^{208}Pb/^{206}Pb$ and $^{207}Pb/^{206}Pb$ were calculated and plotted against each other in a diagram (Fig. 19).

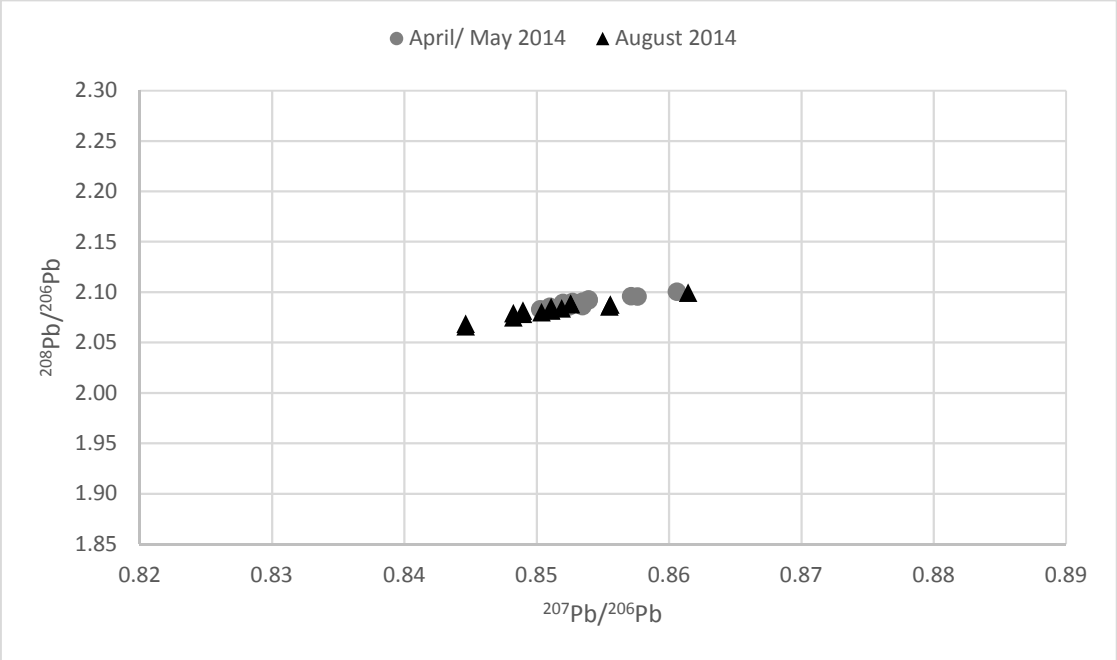

Figure 19: $^{208}Pb/^{206}Pb$-207Pb/206Pb diagram according to the Pb isotope ratios for samples taken in Goiânia

$^{208}Pb/^{206}Pb$ and $^{207}Pb/^{206}Pb$ isotope ratios show significant differences between rainy and dry season. $^{207}Pb/^{206}Pb$ isotope ratios from rainy season are higher than in dry season. The significant variance of $^{207}Pb/^{206}Pb$ ratios between both sampling periods is proved by the consulted Kruskal-Wallis-Test (H= 4.3063, P= 0.0382). $^{208}Pb/^{206}Pb$ ratios demonstrate a highly significant variance between rainy and dry season (H= 8.8716, P= 0.0029) with distinct higher $^{208}Pb/^{206}Pb$ ratios in rainy season, indicating an enrichment of ^{208}Pb isotopes in this period derived from Th-rich environments. In Fig. 20, $^{208}Pb/^{206}Pb$ and $^{207}Pb/^{206}Pb$ isotope ratios from PM in Goiânia were adopted in a Pb-Pb-diagram together with data $^{208}Pb/^{206}Pb$ and $^{207}Pb/^{206}Pb$ isotope ratios from Pb sources taken from the study of Aily (2001). Results are demonstrating the location of Pb isotope ratios from PM in Goiânia in the conformity of isotopic signature of gasoline, exhaust fumes and street dust, indicating a high contribution of traffic

emissions. Furthermore, Pb isotope date from PM in Goiânia are in the range of data from industrial emissions, especially data from dry season with their lower $^{208}Pb/^{206}Pb$ isotope ratios. Hence, industrial emissions also have to be considered as a possible influence factor.

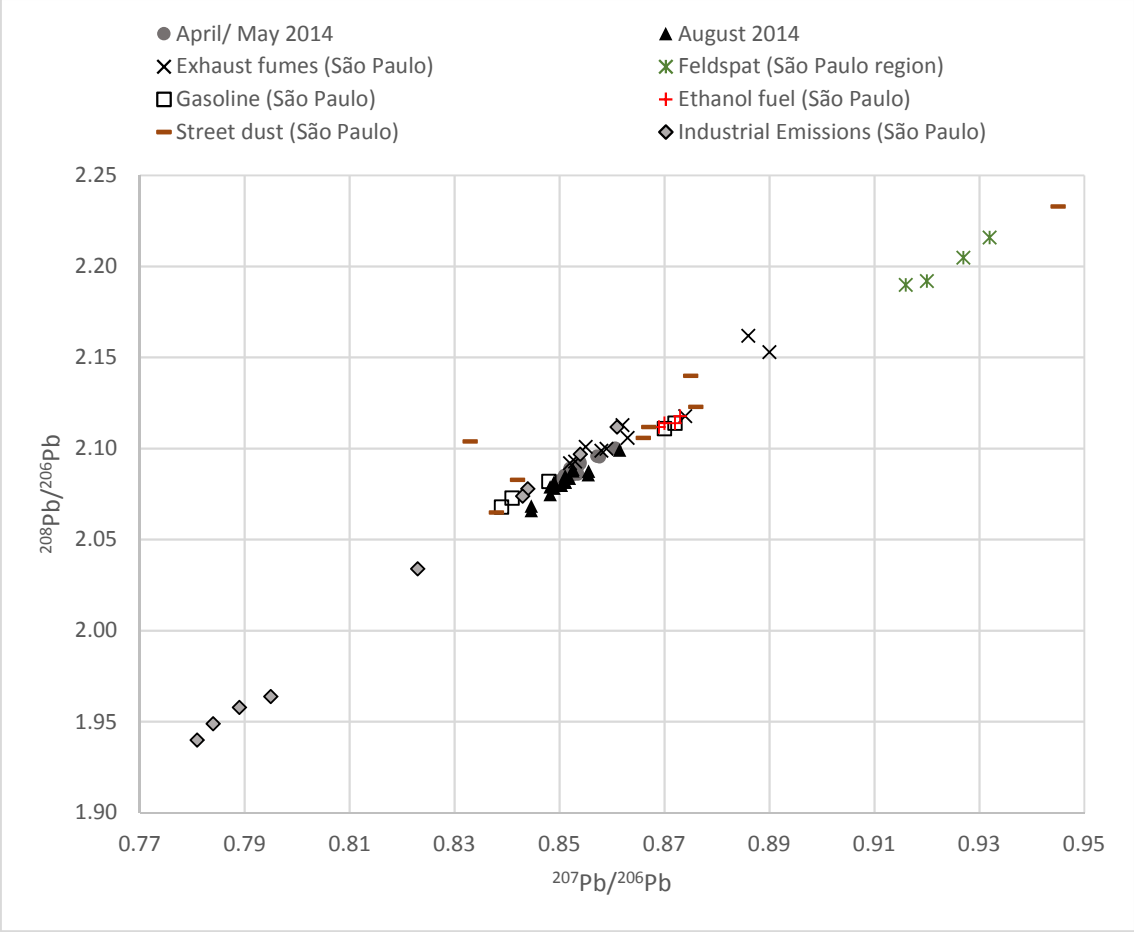

Figure 20: $^{208}Pb/^{206}Pb$-$^{207}Pb/^{206}Pb$ diagram according to the Pb isotope ratios for samples taken in Goiânia compared with Pb isotope ratios from recent studies from Brazil

For a further assessment, $^{206}Pb/^{207}Pb$ isotope ratios of Goiânia samples were plotted together with $^{206}Pb/^{207}Pb$ isotope ratios data from several related studies from Brazil (Fig. 19), as this type of diagram allows to refer on more previous works.

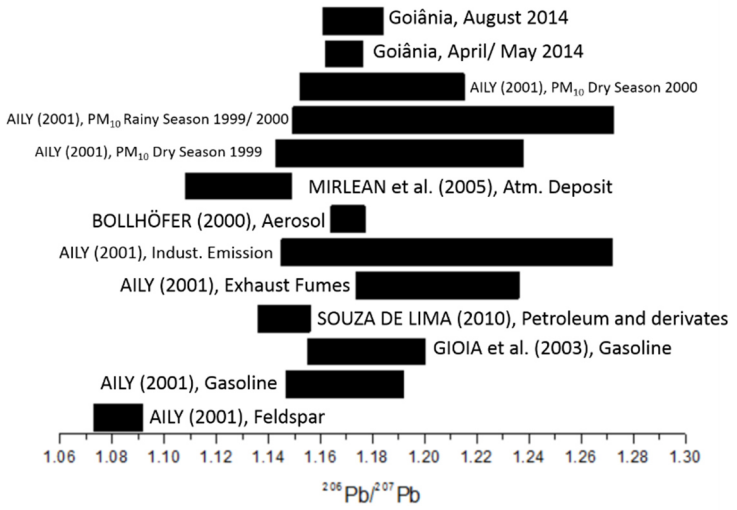

Figure 21: Comparison of the values of $^{206}Pb/^{207}Pb$ isotope ratio here reported with values of recent studies from Brazil

$^{206}Pb/^{207}Pb$ isotope ratios of April/May as well as August samples, are in the range of $^{206}Pb/^{207}Pb$ isotope ratios from PM_{10} samples from São Paulo (Aily, 2001) and aerosol samples from São Paulo (Bollhöfer and Rosman, 2000). Furthermore, the diagram also illustrates, that gasoline and industrial emission, has to be considered as possible Pb sources as both data conform with the $^{206}Pb/^{207}Pb$ isotope ratios from Goiânia.

For a further investigation of the Pb contribution from gasoline and industrial emissions to the Pb of Goiânia samples, the following binary mixing equation was used with the assumption that Pb in both samplings is considered as a mixture between Pb from gasoline and from the industry:

$$R_{PM} = R_{gasoline}X_{gasoline} + R_{industry}X_{industry} \qquad (4)$$

where R_{PM} is the $^{206}Pb/^{207}Pb$ isotope ratios for PM samples, $R_{gasoline}$ and $R_{industry}$ the average $^{206}Pb/^{207}Pb$ isotope ratios for the lead in gasoline and industrial emission, $X_{gasoline}$ the contribution of Pb coming from gasoline in the particulate matter and $1\text{-}X_{gasoline}$ ($=X_{industry}$) the contribution of Pb from industrial emissions in the particulate matter.

The average $X_{gasoline}$ value for samples taken in rainy season was 99.07 ± 7.4 %, while the average $X_{gasoline}$ value for samples taken in dry season was 92.64 ± 10.58 %, showing a very high influence of gasoline on Pb in both

sampling periods. Hence, there is a markedly higher contribution of industrial emission on Pb in dry season samples than on Pb in rainy season samples. Binary mixing equations in order to investigate the contribution of Pb coming from gasoline were also calculated in the works of Zheng et al. (2004) and Mastral et al. (2009), where the contribution factor of gasoline was markedly lower than in this study. In the work of Zheng et al. (2004), contribution of automotive lead on Pb in PM_{10} samples from Shanghai, China, were around 20 %, while the studies of Mastral et al. (2009) resulted in a contribution factor of 23 ± 9 % of Pb coming from gasoline on Pb in PM_{10} samples from Zaragoza, Spain.

5.3 Results and Discussion for Studies in Rio Claro

5.3.1 Elemental Determination of Lead inSamples from Rio Claro

Figures 20 (July), 21 (December) and 22 (February/March) represent the obtained lead concentrations from Rio Claro in ng mL^{-1} in the sample solutions along with the lead concentrations in the respective filter blank solutions and acid blanks. The standard deviation of the lead concentrations of the three main runs is amounted for each sample or blank on the respective bar in the diagram. Instrumental detection limit was identified as 0.0041 ng mL^{-1} and the method detection limit as 0.021 ng mL^{-1}.

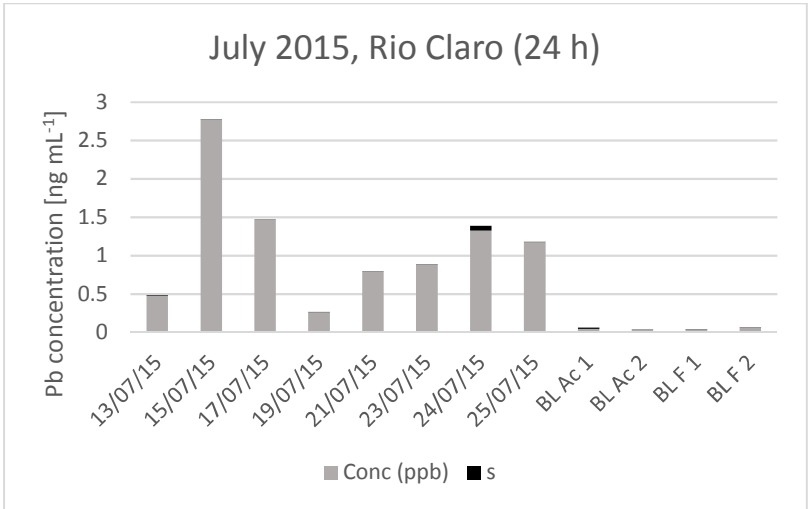

Figure 22: Pb concentrations (Conc.) and respective standard deviations (s) in ng ml^{-1} in sample and blank dilutions of Rio Claro samples from July 2015 (BL Ac = Acid blank, BL F = Filter blank)

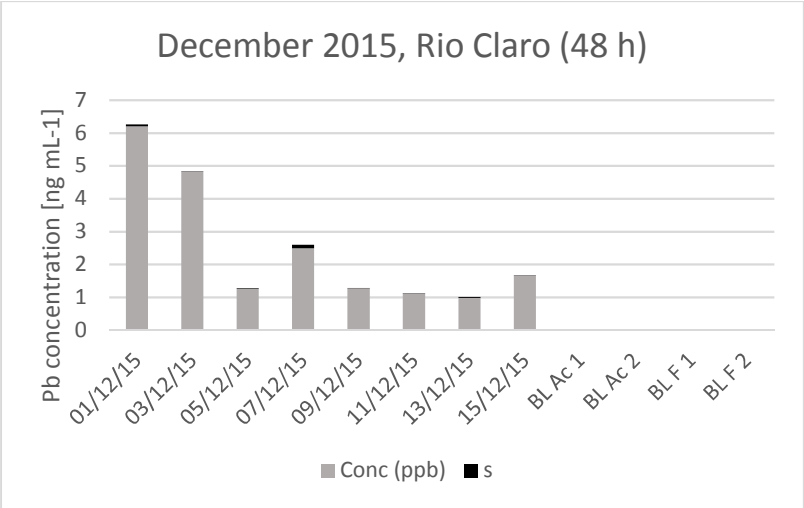

Figure 23: Pb concentrations (Conc.) and respective standard deviations (s) in ng ml^{-1} in sample and blank dilutions of Rio Claro samples from December 2015 (BL Ac = Acid blank, BL F = Filter blank)

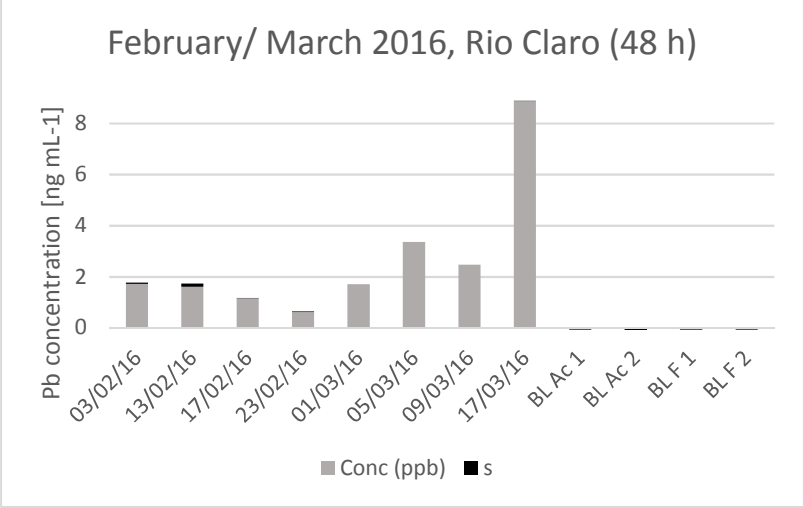

Figure 24: Pb concentrations (Conc.) and respective standard deviations (s) in ng ml^{-1} in sample and blank dilutions of Rio Claro samples from February and March 2016 (BL Ac = Acid blank, BL F = Filter blank)

In figures 23 to 25, lead concentrations per volume of air are represented for the rainy season samples from July 2015, representing dry season, and samples from December 2015 and February/ March 2016, representing rainy season, in Rio Claro.

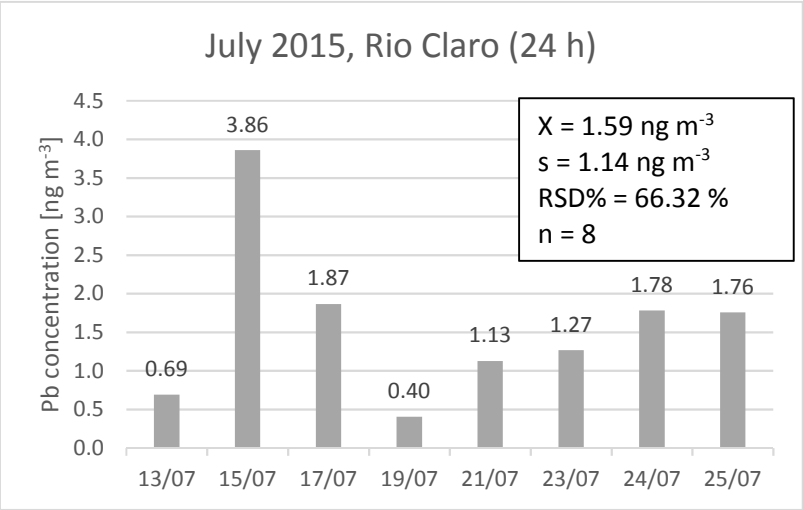

Figure 25: Pb concentration in ng m^{-3} for Rio Claro samples from July 2015 (X = mean value; SD = standard deviation; RSD% = relative standard deviation; n = quantity)

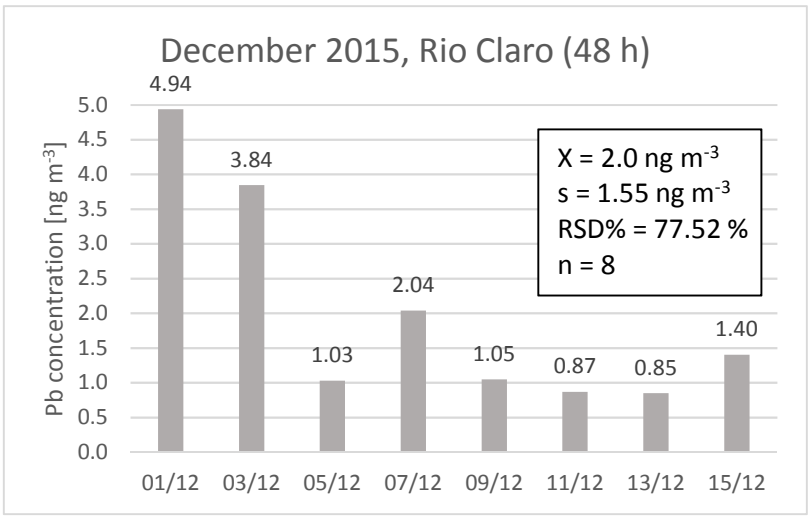

Figure 26: Pb concentration in ng m^{-3} for Rio Claro samples from December 2015 (X = mean value; s = standard deviation; RSD% = relative standard deviation; n = quantity)

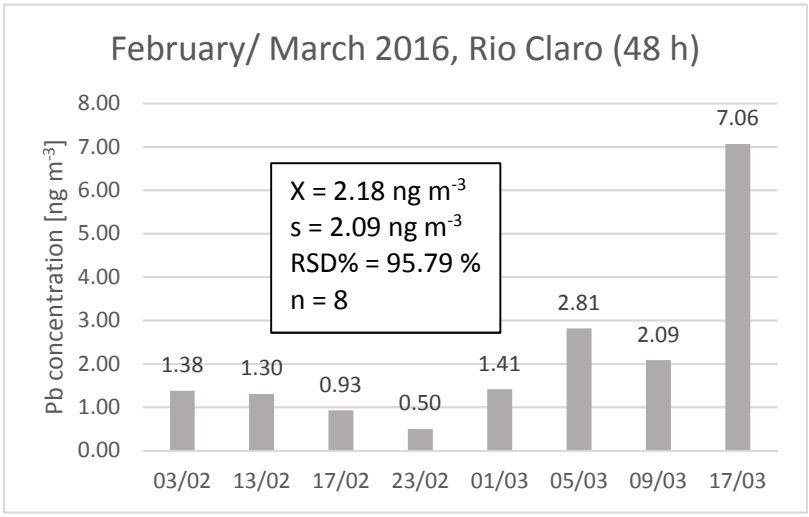

Figure 27: Pb concentration in ng m^{-3} for Rio Claro samples from February and March 2016 (X = mean value; s = standard deviation; RSD% = relative standard deviation; n = quantity)

Pb concentrations from dry season represented by July samples (24 hours of sampling time) differed from 0.40 ng m^{-3} to 3.86 ng m^{-3} with an arithmetic average of 1.59 ng m^{-3} and a relative standard deviation of 71.49 %. Despite the high variance, median and arithmetic average are very close to each other, while asymmetry is highly positive with 1.464 (Table 13). In contrast, samples from December 2015 (48 hours of sampling time) alternate between 0.85 m^{-3} and 4.94 m^{-3}, showing an arithmetic average of 2.00 m^{-3} and a relative standard deviation of 77.52 %. The high variation is also illustrated in the median, which is considerably lower than the arithmetic average. Asymmetry is slightly positive with 1.355. The amplitude of the Pb concentration from February/March samples (48h of sampling time) is between 0.5 ng m^{-3} and 7.06 ng m^{-3}. Concentrations differ highly from each other with a relative standard deviation of 95.79 %. This variance is also shown in the very high difference between arithmetic average (2.18 ng m^{-3}) and median (1.395 ng m^{-3}) and the very high asymmetry of 2.242.

Table 13: Descriptive statistics of rainy season (July 2015) and dry season (December 2015, February/March 2016) samples from Rio Claro

	July 2015 (24h)	December 2015 (48h)	Feb/Mar 2016 (48h)
Sample size	8	8	8
Minimum	0.403	0.850	0.499
Maximum	3.859	4.940	7.064
Total Amplitude	3.456	4.090	6.565
Median	1.513	1.223	1.395
First Quartile (25%)	1.019	0.989	1.208
Third Quartile (75%)	1.803	2.491	2.268
Interquartile Deviation	0.784	1.502	1.060
Arithmetic Average	1.594	2.002	2.185
Variance	1.118	2.409	4.381
Standard Deviation	1.057	1.552	2.093
Standard Error	0.374	0.549	0.740
Coefficient of Variation	66.32%	77.52%	95.79%
Asymmetry	1.464	1.355	2.242

Boxplot diagram (Fig. 26) illustrates that the high outlier value of July samples stretches the arithmetic average to a higher value while median and third quartile are relatively close to each other, so that just two samples are higher than 1.8 ng m^{-3}. As against, in December samples, median and first quartile are close while the disparity between median and third quartile is very high, showing that just two samples have higher Pb concentrations than 2.491 ng m^{-3}. Also in February/March samples, median and first quartile show close values to each other. Noticeable is the high outlier value of 7.06 ng m^{-3}, which lies far distant from third quartile with 2.268 ng m^{-3}, showing the high influence of this outlier on the arithmetic average. So quite similar to December samples, 50 % of February/March samples have a Pb concentration between 1.208 and 2.268 ng m^{-3}.

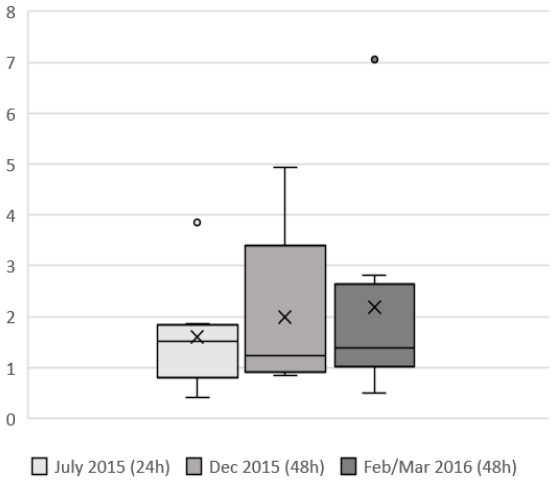

Figure 28: Boxplot diagram for Pb concentrations of rainy (July 2015) and dry season (December 2015, February/March 2016) samples from Rio Claro

To determine the statistical equality of the Pb concentrations between the three sampling periods, a Kruskal-Wallis test was performed by considering all three groups with two degrees of freedom. The test resulted in a H-value of H= 0.285 and a P-value of P= 0.8672, which shows a high statistical equality between the sampling groups. An executed Kruskal-Wallis test considering just the sampling periods of December and February/March showed a H-value of 0.0993 and P-value of 0.7527, which also indicates a highly statistical equality between the Pb concentrations of this two sampling groups.

Compared to other studies measuring Pb concentrations in particulate matter (as mentioned in *5.2.1*), Pb concentrations from Rio Claro samples are relatively low. In this study location, also no sample exceeded the guide values established by CETESB, the European Union or United States Environmental Protection Agency.

5.3.2 Back Trajectory Analysis of Sampling Point in Rio Claro

In order to assess directions of air masses and hence possible sources of lead in Rio Claro samples, back trajectories with a run time of 24 hours were calculated for sampling dates in rainy dry season with markedly elevated (higher than median) and low concentration levels (lower than median) of Pb. For samples of rainy season, back trajectories had a run time of 48 hours and sampling days with elevated Pb concentrations were selected as days with Pb

concentrations higher than or near 75 % quartile and sampling days with low Pb concentrations as days with Pb concentrations lower than or near 25 % quartile. Trajectory plots ended respectively at the end of each sampling date at three different heights (0 m, 100 m, 250 m AGL).

Air masses arriving in Rio Claro at dates with elevated Pb concentrations in dry season (15th, 17th, 24th and 25th July) mainly came from very low altitudes under 100 m AGL from north east direction, originated in the mountain ridges in the south of Minas Gerais (Fig. 27). Just on 25th July 2015 sampling point received air masses from high altitudes of up to 1100 m which came from western direction before they turned to north-east to pass the city of Santa Gertrudes to arrive in Rio Claro.

Back trajectory models for days with low Pb concentrations in dry season (13th, 19th, 21st and 23rd July) show that also in this period most of air masses arriving at the sampling point came from north-east direction, but here showing a high alternation of the passed altitudes above ground level (Fig. 28). In contrast air masses arriving on 21th July 2015 at sampling point came from north-west with the origin of inner São Paulo state before they turned and arrived over Santa Gertrudes coming from south-east to Rio Claro.

48 hours back trajectories of sampling dates with high Pb concentrations in rainy season (1st and 3rd December, 5th and 17th March) demonstrate that a part of air masses came from the south-west (1st and 3rd December), coming from north-east Parana and travelling at high altitudes up to 3000 m AGL parallel to the coast mountains of Serra de Paranapiacaba and after northwards to Rio Claro. Other air masses (5th March) arrived from the north travelling in very low altitudes less than 200 m and from eastern direction, originated in the south of Minas Gerais and passing in highly descending altitudes from 1500 m AGL downwards (Fig. 29).

In rainy season on days with low Pb concentrations, air masses arrived from sampling point from north/ north-east (5th and 11th December, 17th and 23rd February), travelling in low altitudes up to 500 m AGL, or coming from west/ north-west (5th December, 17th February) directed from the interior of São Paulo State, where they passed through alternating heights between 0 and 1000 m AGL (Fig. 30).

Back trajectory models from the sampling point in Rio Claro demonstrate that in dry season most of the air masses come from north-east direction on days with elevated Pb concentrations as well as on days with lower Pb concentrations. Thus, lead concentrations in dry season seem to be independent from air mass directions in this period. But a factor of influence here could be the height level of air masses. Hence, air masses arriving at sampling point on days with high Pb concentrations passed low altitudes near ground level, while on days with low Pb concentrations, air masses originated from high altitudes passing heights to 1000 and up to 1500 m. In rainy season no trend is visible, which also indicates the independency of lead concentration levels on air mass directions in this period. Therefore, the assumption that air masses have a low influence on Pb in Rio Claro and Pb in Rio Claro is probably contributed by local Pb sources, is supported.

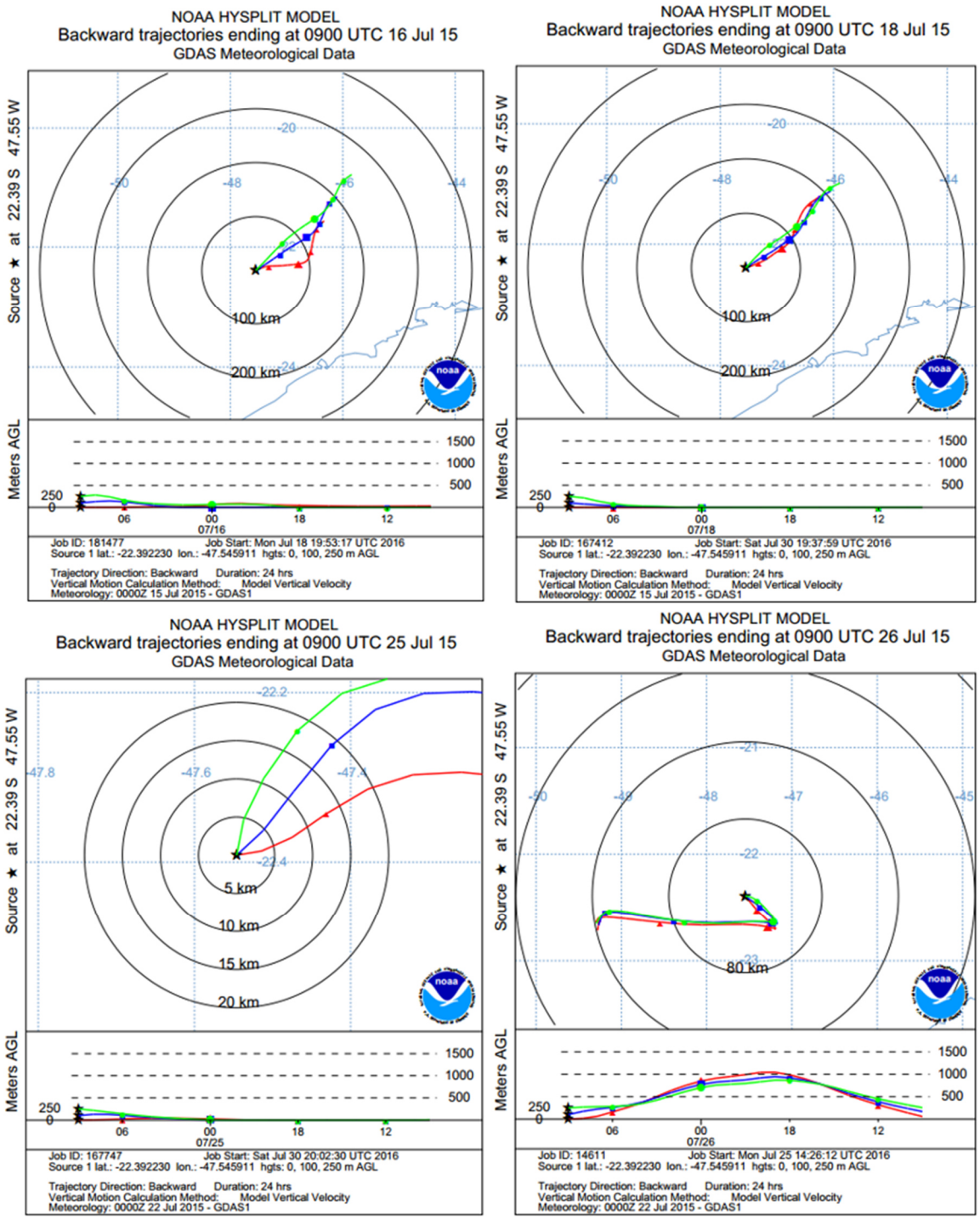

Figure 29: Back trajectory plots ending at three different height levels (0 m; 100 m; 250 m AGL) on episodic dates with elevated Pb concentrations in dry season arriving at sampling point in Rio Claro

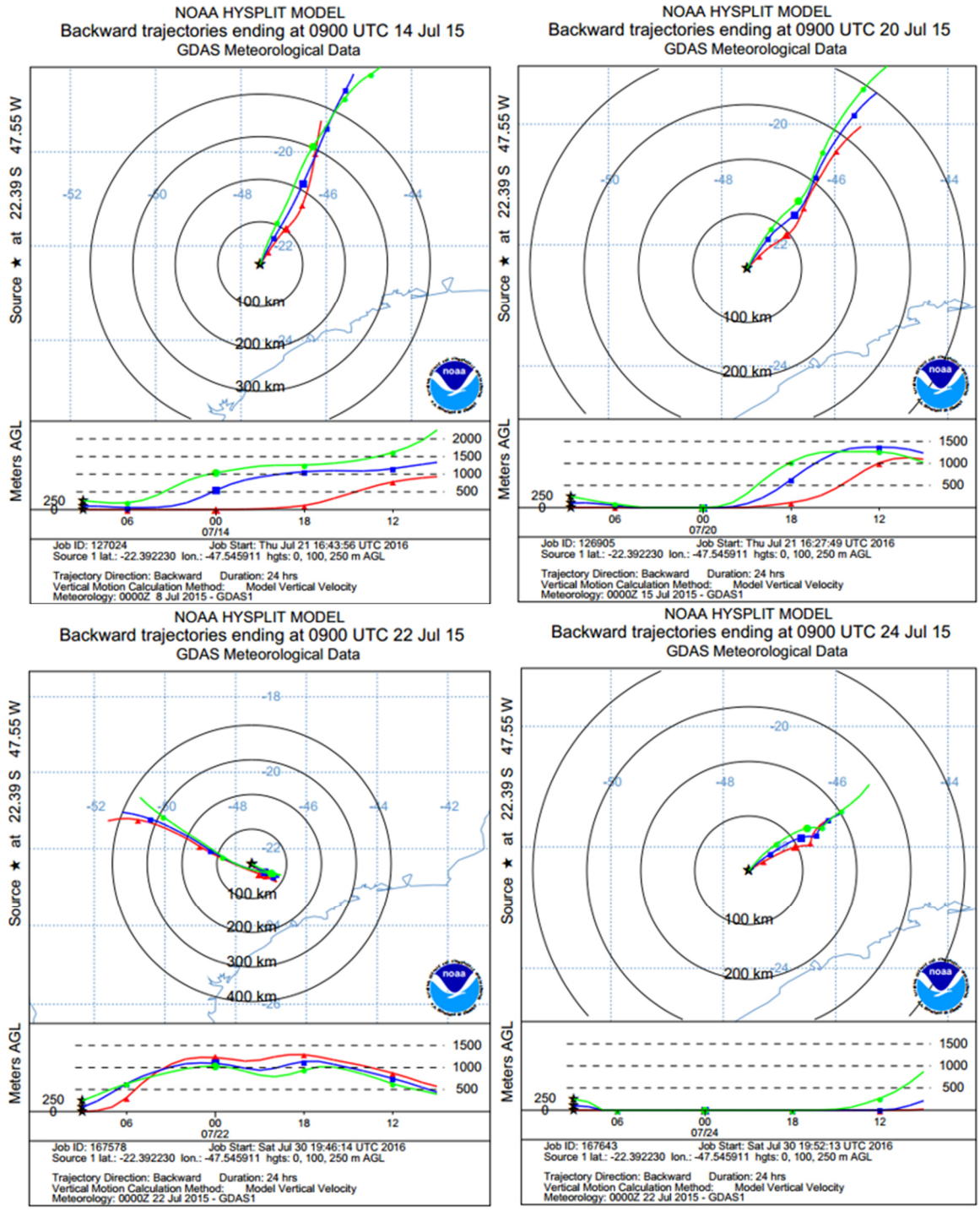

Figure 30: Back trajectory plots ending at three different height levels (0 m; 100 m; 250 m AGL) on episodic dates with low Pb concentrations in dry season arriving at sampling point in Rio Claro

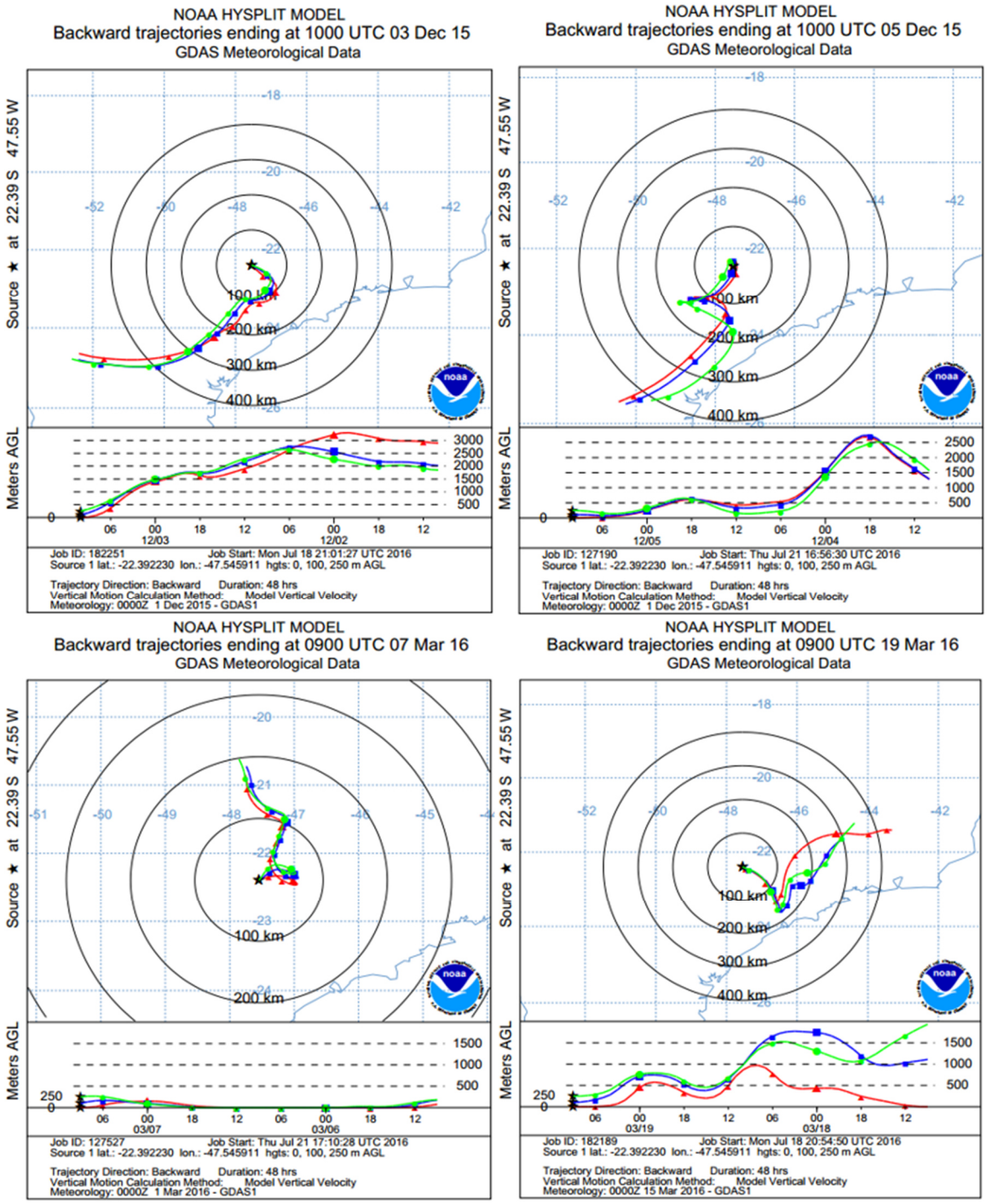

Figure 31: Back trajectory plots ending at three different height levels (0 m; 100 m; 250 m AGL) on episodic dates with elevated Pb concentrations in rainy season arriving at sampling point in Rio Claro

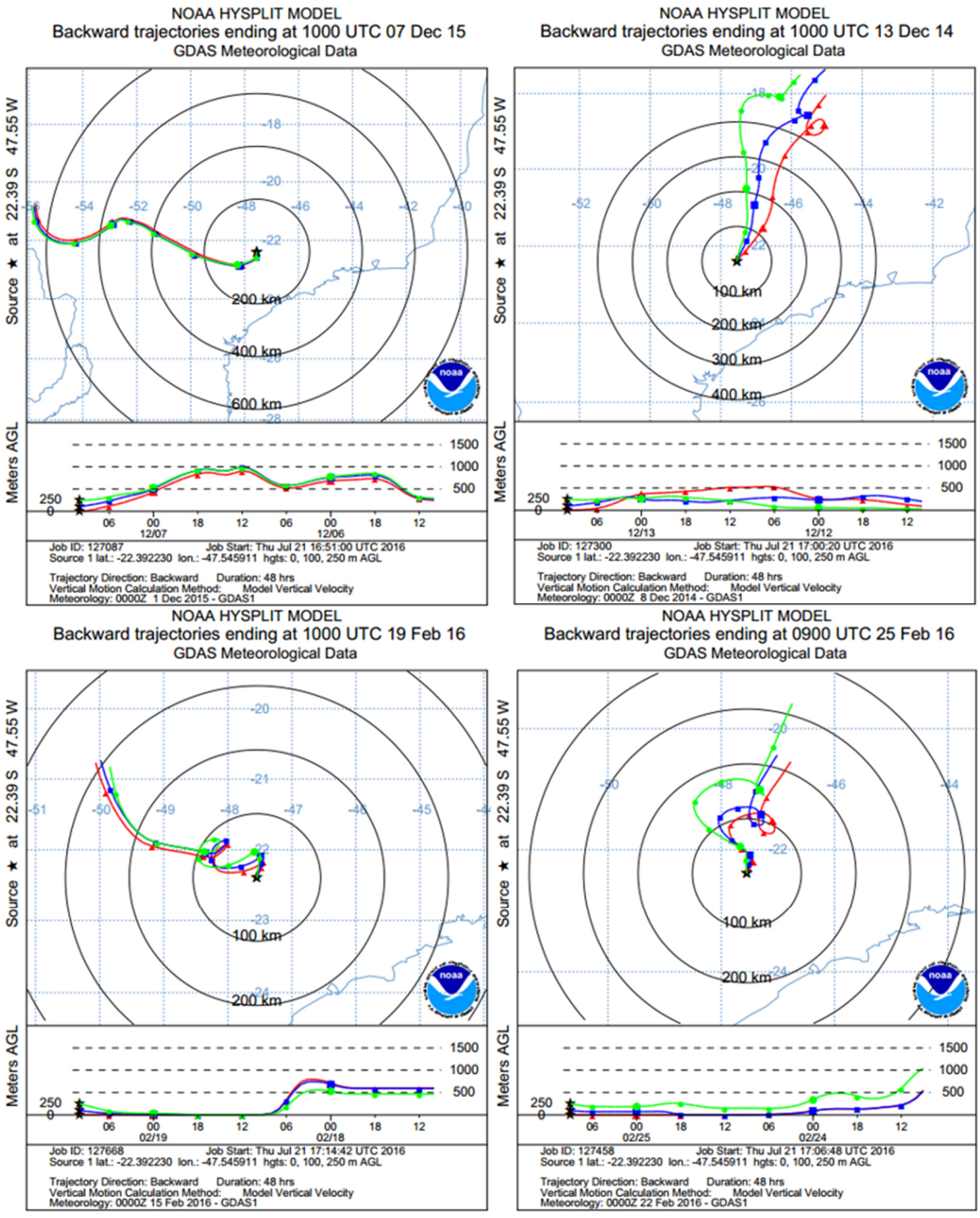

Figure 32: Back trajectory plots ending at three different height levels (0 m; 100 m; 250 m AGL) on episodic dates with low Pb concentrations in rainy season arriving at sampling point in Rio Claro

5.3.3 Isotopic Determination of Lead in Samples from Rio Claro

The tables 14 and 15 show the mass bias corrected $^{206}Pb/^{207}Pb$ and $^{208}Pb/^{207}Pb$ isotope ratios with the afore mentioned equation (2) for Rio Claro samples along with their relative standard deviations (RSD) for three main analysing runs.

Table 14: Corrected lead isotope ratios of Rio Claro samples from dry season (July 2015) with their relative standard deviations (X = mean value; s = standard deviation; RSD% = relative standard deviation)

Date	$^{206}Pb/^{207}Pb$	RSD%	$^{208}Pb/^{207}Pb$	RSD%
13/07/2015	1.1750	0.299	2.4515	0.112
15/07/2015	1.1740	0.142	2.4505	0.068
17/07/2015	1.1760	0.298	2.4525	0.145
19/07/2015	1.1740	0.181	2.4446	0.227
21/07/2015	1.1730	0.027	2.4505	0.262
23/07/2015	1.1952	0.203	2.4664	0.122
24/07/2015	1.1750	0.125	2.4436	0.089
25/07/2015	1.1700	0.145	2.4495	0.166
X	1.1765	0.178	2.4511	0.149
s	0.0078		0.0070	
RSD%	0.6593		0.2845	

Table 15: Corrected lead isotope ratios of Rio Claro samples from rainy season (December 2015 and February/ March 2016) with their relative standard deviations (X = mean value; s = standard deviation; RSD% = relative standard deviation)

Date	$^{206}Pb/^{207}Pb$	RSD%	$^{208}Pb/^{207}Pb$	RSD%
01/12/15	1.1816	0.020	2.4591	0.029
03/12/15	1.1635	0.024	2.4412	0.054
05/12/15	1.1696	0.095	2.4511	0.041
07/12/15	1.1816	0.227	2.4402	0.145
09/12/15	1.1645	0.153	2.4402	0.063
11/12/15	1.1635	0.049	2.4432	0.081
13/12/15	1.1696	0.167	2.4442	0.120
15/12/15	1.1696	0.152	2.4462	0.022
03/02/16	1.1709	0.136	2.4567	0.110
13/02/16	1.1689	0.188	2.4517	0.214
17/02/16	1.1669	0.120	2.4537	0.064
23/02/16	1.1570	0.240	2.4527	0.161
01/03/16	1.1635	0.061	2.4394	0.216
05/03/16	1.1585	0.084	2.4374	0.073
09/03/16	1.1645	0.074	2.4444	0.053
17/03/16	1.1635	0.044	2.4434	0.068
X	1.1673	0.115	2.4465	0.095
s	0.0068		0.0067	
RSD%	0.5841		0.2736	

In the measured $^{206}Pb/^{207}Pb$ isotope ratio data of dry season samples, two RSD values are higher than 0.2 %, while $^{208}Pb/^{207}Pb$ isotope ratio data show a similar precision with also two RSD values over 0.2 %. In contrast, rainy season samples show a higher precision with two RSD values over 0.2 % in the $^{206}Pb/^{207}Pb$ isotope ratio data and two with RSD <0.2 % in the $^{208}Pb/^{207}Pb$ isotope ratio data.

To compare Pb isotope ratio data from the three sampling periods, $^{206}Pb/^{207}Pb$ and $^{208}Pb/^{207}Pb$ isotope ratios were plotted in a Pb-Pb diagram (Fig. 31).

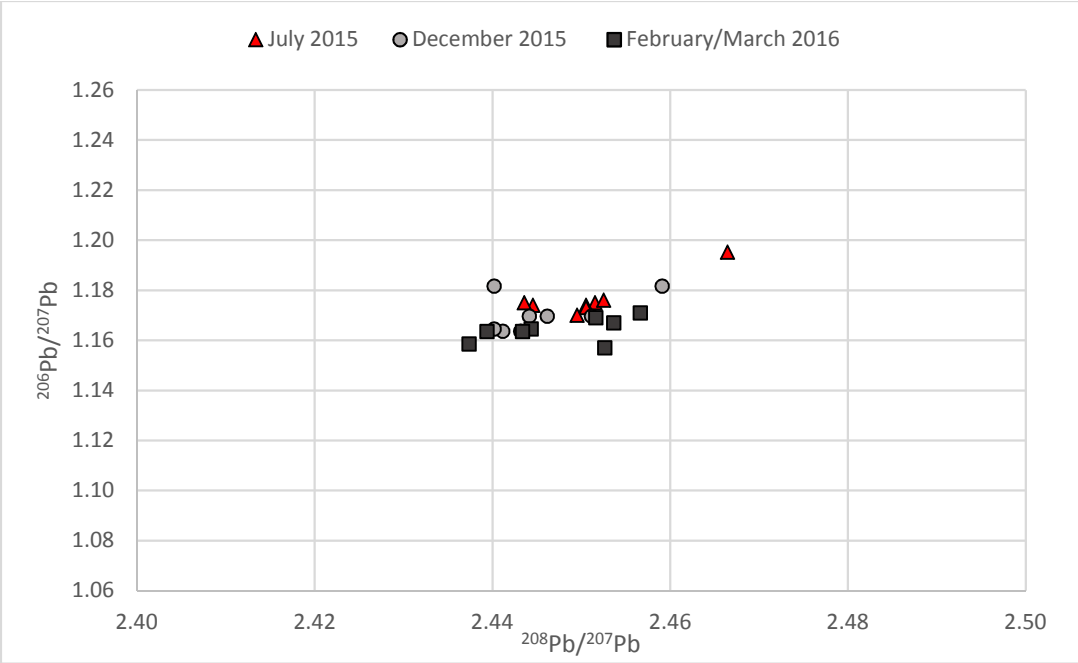

Figure 33: Pb–Pb diagram according to the Pb isotope ratios for samples taken in Rio Claro

The $^{206}Pb/^{207}Pb$ isotope ratios varied in the dry season samples from 1.1700 to 1.1952, while $^{208}Pb/^{207}Pb$ isotope ratios differed from 2.4436 to 2.4664. The $^{206}Pb/^{207}Pb$ isotope ratios from samples representing rainy season (December 2015, February/March 2016) differed from 1.157 to 1.1816 and $^{208}Pb/^{207}Pb$ isotope ratios from 2.4374 to 2.4591. Arithmetic averages of $^{206}Pb/^{207}Pb$ isotope ratios of dry season samples are higher (1.1765) than rainy season samples (1.1673). $^{208}Pb/^{207}Pb$ ratios are also higher in dry season (2.4511) than in rainy season (2.4466).

Variance of Pb isotope ratios is slightly higher in dry season samples (coefficient of variation of 0.66 % for $^{206}Pb/^{207}Pb$ isotope ratios and 0.28 % for $^{208}Pb/^{207}Pb$ ratios) than in rainy season (coefficient of variation of 0.58 % for $^{206}Pb/^{207}Pb$ isotope ratios and 0.27 % for $^{208}Pb/^{207}Pb$ ratios). For the assessment of the statistical difference of Pb isotope ratios between both sampling periods, a Kruskal-Wallis test was performed. The analysis of the $^{206}Pb/^{207}Pb$ isotope ratios between both sampling groups resulted in H= 9.0748 with P= 0.0027, demonstrating a very high disparity between both sample periods. The outcome of the performed test for $^{208}Pb/^{207}Pb$ isotope ratios were H= 1.6552 with P= 0.1983, which illustrates that there is no identifiable disparity between $^{208}Pb/^{207}Pb$ isotope ratios of both sampling groups. Hence, $^{208}Pb/^{207}Pb$

isotope ratios from dry season are located in the range of $^{208}Pb/^{207}Pb$ isotope ratios from rainy season, whereas $^{206}Pb/^{207}Pb$ isotope ratios in dry season samples show higher values than in rainy season samples. Higher $^{206}Pb/^{207}Pb$ isotope ratios in dry season indicate to an enrichment of ^{206}Pb isotopes in this period.

In order to assess possible emission sources, measured $^{208}Pb/^{207}Pb$ and $^{206}Pb/^{207}Pb$ isotope ratios were plotted on a Pb-Pb diagram (Fig. 32) together with data from previous studies from Brazil, which contain Pb isotope ratios of aerosol samples from São Paulo (Bollhöfer and Rosman, 2000), gasoline, industrial emission and exhaust fume samples from São Paulo (Aily, 2001) and atmospheric deposit samples from Rio Grande (Mirlean et al., 2005).

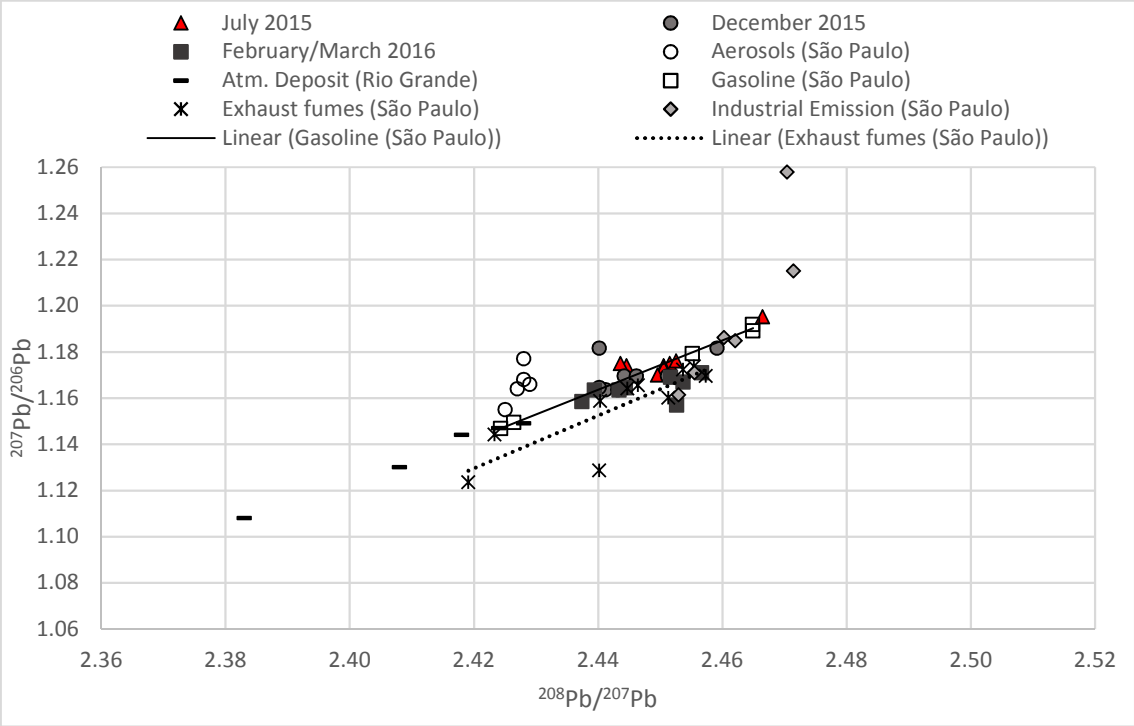

Figure 34: Pb–Pb diagram according to the Pb isotope ratios for samples taken in Rio Claro compared with Pb isotope ratios from recent studies from Brazil

Pb isotope ratios in aerosol samples from São Paulo and atmospheric deposit samples from Rio Grande show high differences from Pb isotope ratios in Rio Claro samples. Pb isotope ratios of dry season and rainy season samples from Rio Claro are distributed on the line of gasoline Pb concentrations from São Paulo. Hence, also here gasoline is seeming to be a major factor of influence on Pb of Rio Claro samples. This presumption is also supported by

the distribution of the Pb isotope ratio data of exhaust fumes from São Paulo near Pb isotope ratio data from Rio Claro samples. Due to the higher $^{206}Pb/^{207}Pb$ isotope ratios values of dry season samples, Pb isotope ratio data of this sampling period is nearer to the Pb isotope ratios of industrial emissions from São Paulo. This can be an indicator that Pb in dry season is also influenced by industrial emissions.

In order to investigate the contribution from the decay of Thorium to the Pb in PM in Goiânia, ratios of $^{208}Pb/^{206}Pb$ and $^{207}Pb/^{206}Pb$ were calculated and plotted against each other in a diagram (Fig. 35).

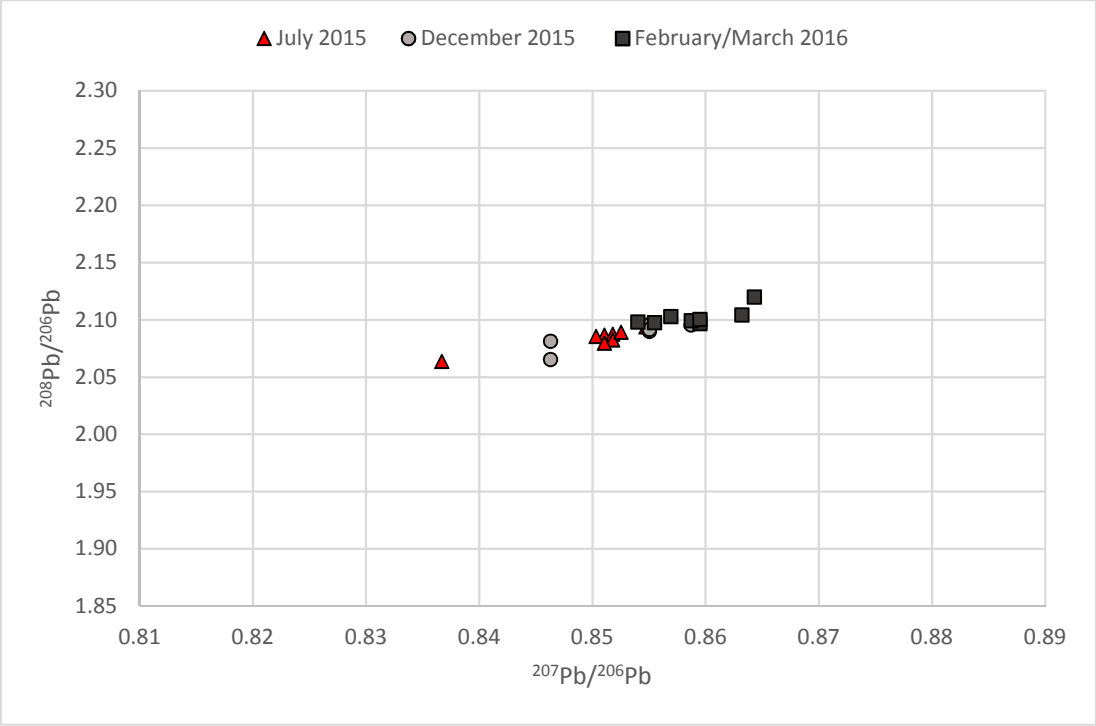

Figure 35: $^{208}Pb/^{206}Pb$-$^{207}Pb/^{206}Pb$ diagram according to the Pb isotope ratios for samples taken in Goiânia

$^{208}Pb/^{206}Pb$ and $^{207}Pb/^{206}Pb$ isotope ratios show significant differences between rainy and dry season. Performed Kruskal-Wallis-Test along with post-hoc tests show that sampling groups from dry and rainy season differ significantly from each other in their $^{208}Pb/^{206}Pb$ isotope ratios (H= 9.0077, P= 0.0027) and $^{207}Pb/^{206}Pb$ isotope ratios (H= 9.0391, P= 0.0027). Especially data from February/March 2016 is responsible for this disparity as $^{208}Pb/^{206}Pb$ and $^{207}Pb/^{206}Pb$ isotope ratios show markedly higher values than data from July 2015 and December 2015. This observation indicates an enrichment of ^{208}Pb

isotopes and ^{207}Pb isotopes in the sampling period of February/March 2016. In Fig. 36, $^{208}Pb/^{206}Pb$ and $^{207}Pb/^{206}Pb$ isotope ratios from PM in Goiânia were adopted in a Pb-Pb-diagram together with data $^{208}Pb/^{206}Pb$ and $^{207}Pb/^{206}Pb$ isotope ratios from Pb sources taken from the study of Aily (2001). Results demonstrate that $^{208}Pb/^{206}Pb$ and $^{207}Pb/^{206}Pb$ isotope ratios from PM in Rio Claro conform with the range of the isotopic signature of gasoline, exhaust fumes and street dust. This indicates, such as Fig. 34, that main contribution factor for Pb in PM in Rio Claro are traffic emissions. Furthermore, Pb isotope data from PM in Rio Claro is placed in the range of data from industrial emissions, especially data from July 2015 and December 2015 due to their lower $^{208}Pb/^{206}Pb$ isotope ratios. Thus, industrial emissions also have to be considered as a possible influence factor for Pb in PM in this sampling periods.

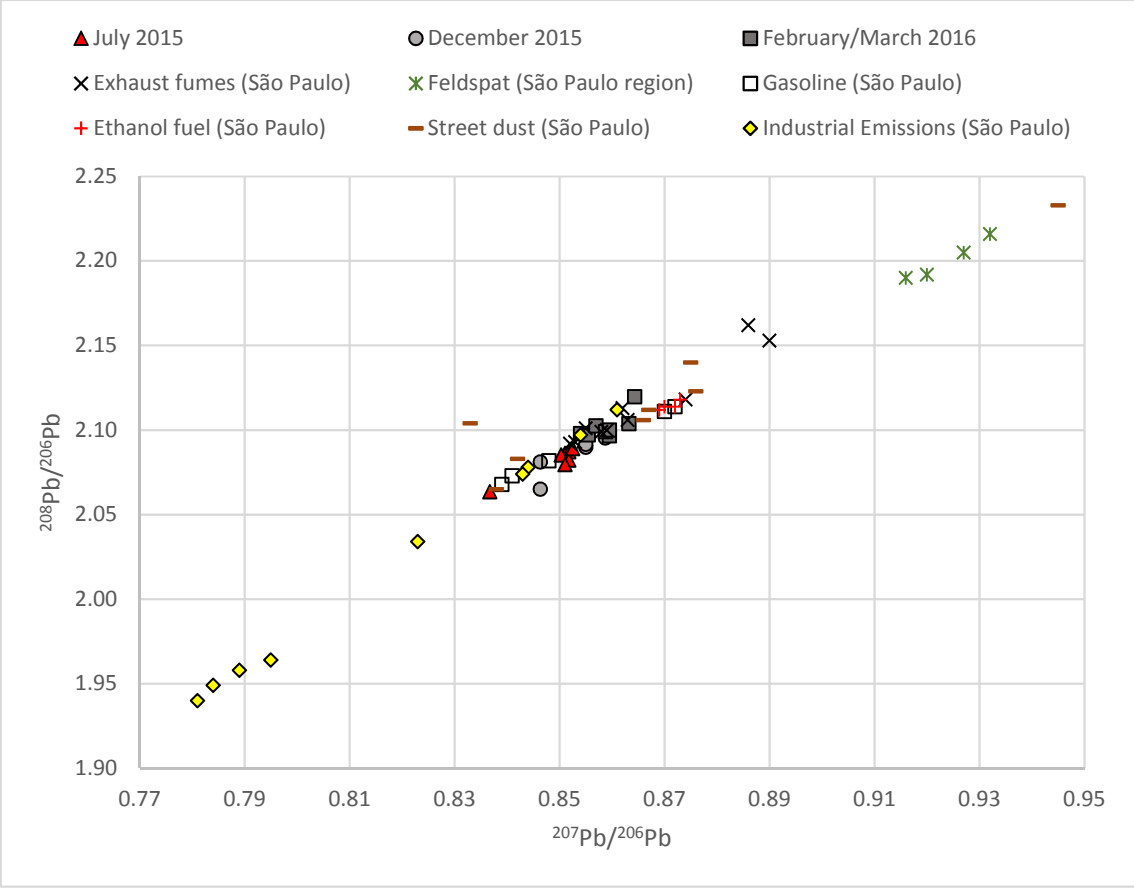

Figure 36: $^{208}Pb/^{206}Pb$-$^{207}Pb/^{206}Pb$ diagram according to the Pb isotope ratios for samples taken in Rio Claro compared with Pb isotope ratios from recent studies from Brazil

For a further assessment, $^{206}Pb/^{207}Pb$ isotope ratios of Rio Claro samples were plotted together with $^{206}Pb/^{207}Pb$ isotope ratios data from several related

studies from Brazil (Fig. 33), as this type of diagram allows to refer on more previous works.

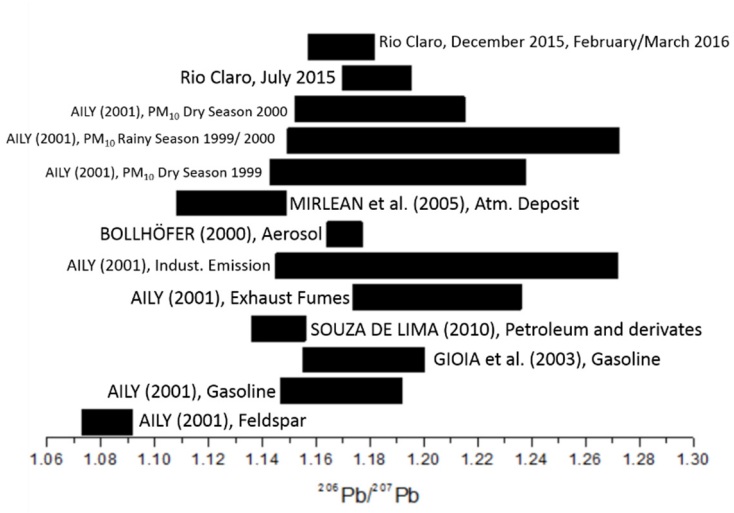

Figure 37: Comparison of the values of $^{206}Pb/^{207}Pb$ isotope ratio here reported with values of recent studies from Brazil

$^{206}Pb/^{207}Pb$ isotope ratios of dry season as well as of rainy season are according with $^{206}Pb/^{207}Pb$ isotope ratios from PM_{10} samples from São Paulo (Aily, 2001) and aerosol samples from São Paulo (Bollhöfer and Rosman, 2000). Furthermore, both sample periods conform with the range of gasoline and industrial emission from São Paulo. Also in this diagram, the higher $^{206}Pb/^{207}Pb$ isotope ratios of dry season samples are illustrated, indicating a possible higher influence of industrial emissions on Pb in dry season in Rio Claro.

A binary mixing equation as described above (Calculation 4) was applied for a further assessment of Pb contribution from gasoline and industrial emissions to the Pb of Rio Claro samples with the assumption that Pb in both samplings is considered as a mixture between Pb from gasoline and from the industry.

Calculations resulted in an average $X_{gasoline}$ value of 89.68 ± 14.25 % for samples taken in dry season and an averaged $X_{gasoline}$ value of 107.8 ± 12.97 % for samples taken in rainy season. Thus, Pb in samples from rainy season seems to be totally contributed from gasoline, while Pb in samples from dry season are highly influenced by Pb from gasoline, but also industrial emission seems to be an influence factor in minor part for the Pb in this sampling period. The high $X_{gasoline}$ results over 100 % show that other potential Pb sources

besides traffic and industrial emissions has to considered as contribution factors to Pb in Rio Claro.

6 Conclusion

Basic methods using ICP-MS technique in matters of optimization of acquisition time and dead time as well as the correction of mass bias were successfully implemented, which allowed an accurate and precise direct determination of Pb isotope ratios of the study samples.

Lead concentrations from Goiânia showed difference between rainy and dry season. Samples from August, representing dry season, had higher Pb concentration values in average and varied in a lower scope than samples from April/May, representing rainy season. In Rio Claro, Pb concentrations showed a lower variance in dry season than samples from rainy season, whereas Pb concentrations between dry and rainy season were quite similar. For both cities, no date exceeded the guide values established by CETESB, the European Union or United States Environmental Protection Agency. Back trajectory evaluation in Goiânia demonstrated that in rainy season on days with elevated lead concentrations air masses came prevailingly from eastern direction. In contrast to that, whereas on days with lower Pb concentrations in dry season air mass directions showed the trend to come from eastern direction. In Rio Claro, lead concentrations in dry season and rainy season seemed to be independent from air mass directions, indicating local Pb sources as main contribution factor.

Lead isotope ratio analysis showed that Pb in Goiânia samples was highly influenced by traffic emissions. However, there were slight differences in Pb isotope ratios between dry and rainy season as Pb from dry season seems to be also influenced by industrial emissions. Also in Rio Claro, main contribution factor to Pb in study samples were traffic emissions, whereas in dry season also an influence of industrial emissions was determinable. But results from binary mixing equations illustrated that also other Pb sources has to be considered as potential factor of influence to Pb in Goiania and Rio Claro. Hence, data sets of lead sources in Brazil are fragmentary and more data of possible Pb sources has to be consulted, in order to develop a more significant assessment.

7 References

AILY, C. Caracterização isotópica de Pb na atmosfera: Um exemplo da cidade de São Paulo. Dissertação de Mestrado, Instituto de Geociências, USP, São Paulo, 76 p, 2002.

ALMEIDA, F. F. M. Fundamentos Geológicos do relevo paulista. Boletim IGG, São Paulo, n. 41, 1p. 69-263, 1964.

ALVARES, C.A.; STAPE, J. L.; SENTELHAS, P. C.; GONÇALVES, J. L. DE M. SPAROVEK, G. Köppen Climate Classification map for Brazil. Meteorologische Zeitschrift. Vol 22, n°6, p 711-728, 2005.

ASPACER (Associação Paulista das Cerâmicas de Revestimento). Revista Ano III, numero 27, 2011.

BABINSKI, M. Pb isotopic signatures of the atmosphere of the São Paulo city, Brazil. Journal de physique. IV [1155-4339], pg: 87 -90, 2003.

BECKER, J. S., DIETZE H. J. Ultratrace and precise isotope analysis by double focusing sector field inductively coupled plasma mass spectrometry. J. Anal. At. Spectrom. 13(9), 1057, 1998

BELLIS, D.J.; SATAKE, K.; INAGAKI, M.; ZENG, J., OIZUMI, T. Science of the Total Environment, 341, 149–158, 2005.

BOLLHÖFER, A.; ROSMAN, K.J.R. Isotopic Source Signatures for Atmospheric Lead: The Southern Hemisphere. Geochimica et Cosmochimica Acta, 64, 3251-326, 2000.

BOLLHÖFER, A.; ROSMAN, K.J.R. Isotopic Source Signatures for Atmospheric Lead: The Northern Hemisphere. Geochimica et Cosmochimica Acta, 65, 1727-1740, 2001.

CASTANHO, A.; ARTAXO, P. Wintertime and summertime São Paulo aerosol source apportionment study. Atmospheric Environment v. 35, p. 4889-4902, 2001.

COMPANHIA AMBIENTAL DO ESTADO DE SÃO PAULO (CETESB), Diretoria de Engenharia e Qualidade Ambiental, Departamento de Qualidade Ambiental, Divisão de Qualidade do Ar, EQQA / EQQM / EQQT, Operação Inverno – 2013, Qualidade Do Ar, Janeiro/2014, 2014.

CONAMA Nº 003 (1990) – Conselho Nacional de Meio Ambiente. Dispõe sobre padrões de qualidade do ar, previstos no PRONAR. Resolução CONAMA n. 03, de 28 de junho de 1990.

COTTAS, L. R. Estudos geológico-geotécnicos aplicados ao planejamento urbano de Rio Claro- SP. São Paulo, SP. 171 f., 2V. (Tese de Doutoramento) – Instituto de Geociências/ USP – São Paulo, 1983.

DANNI, J. C. M.; FUCK, R. A.; LEONARDOS, O. H. Archaean and Lower Proterozoic units in central Brazil. Geologische Rundschau, v. 71, n. 1, p. 291-317, 1982.

DRAXLER, R.R., ROLPH, G.D. HYSPLIT (HYbrid SingleParticle Lagrangian Integrated Trajectory) Model access via NOAA ARL READY./http://www.arl.noaa.gov/ready/hysplit4.htmlS. NOAA Air Resources Laboratory, Silver Spring, MD. 2003

Directive 98/70/EC of the European Parliament and of the Council of 13th October 1998 related to the quality of petrol and diesel fuels and amending directive 93/12/EEC.

FUCK, R.A.; MARINI, O.J. O Grupo Araxá e unidades homotaxiais. Symposium about São Francisco craton and their marginal belts, Salvador, 1 (1981), pp.

118–130 (Abstract Volume), 1981.

FLAMENT, P.; BERTHO, M.L.; DEBOUDT, K.; VERON, A.; PUSKARIC E. European isotopic signatures for lead in atmospheric aerosols: a source apportionment based upon $^{206}Pb/^{207}Pb$ ratio. Science of the Total Environment, 296, 35–37, 2002.

GODISH, T. Air quality. Boca Raton: CRC Press, LLC, 1997.

GIOIA, S.M.C.L.; PIMENTEL, M.M.; GUIMARÃES, E.M.; CAMPOS, J.E.L.; DANTAS, E.L.; MARUOKA, M.T.S. Atmospheric Deposition and Sources of Anthropogenic Lead in Sediments from an Artificial Lake in Brasilia, Central Brazil. Proceedings of the IV South American Symposium on Isotope Geology, Salvador-Bahia, 24-27 August 2003, 434-437, 2003.

Governo de Goiás – Internet presence: http://www.goias.gov.br/paginas/conheca-goias/aspectos-fisicos/clima, 2016.

HOPKE, P. K. An Introduction to Receptor Modeling. In: HOPKE, P. K. (Ed.) Receptor modeling for air quality management. USA, New York: Elsevier, cap. 1, p. 1-10, 1991.

INSTITUTO DE PESQUISAS TECNOLÓGICAS DO ESTADO DE SÃO PAULO-IPT Mapa geomorfológico do Estado de São Paulo- escala 1:1000.000. São Paulo. (IPT. Série Monografias), 1981.

JACOBSON, M. Z. Atmospheric Pollution – History, Science and Regulation, Cambridge University Press, 2002.

JARVIS, K.E., GRAY, A.L. Handbook of Inductively Coupled Plasma Mass Spectrometry, Blackie, Glasgow, ch. 11, p. 312, 1992.

KNOLL, G. F. Radiation Detection and Measurement, John Wiley & Sons,

Chichester, 2000, ch. 4, pp. 119–122.

KYOTANI, T., IWATSUKI, M. Characterization of soluble and insoluble components in $PM_{2.5}$ and PM_{10} fractions of airborne particulate matter in Kofu city, Japan. Atmospheric Environment 36, 639–649, 2002.

LEE, C., LI, X.-D., ZHANG, G., LI, J., DING, A.-J., WANG, T. Heavy metals and Pb isotopic composition of aerosols in urban and suburban areas of Hong Kong and Guangzhou, South China—Evidence of the long-range transport of air contaminants. Atmospheric Environment 41, 432-447, 2007.

LEE, S. Fine particulate matter measurement and international standardization for air quality and emissions from stationary sources. Fuel v. 89, p. 874-882, 2010.

LEE, P.-K., JO H. Y., KANG, M.-J., KIM, S.-O. Seasonal variation in trace element concentrations and Pb isotopic composition of airborne particulates during Asian dust and non-Asian dust periods in Daejeon, Korea. Environmental Earth Science 74:3613–3628, 2015.

LEWTAS, J. Air pollution combustion emissions: Characterization of causative agents and mechanisms associated with cancer, reproductive, and cardiovascular effects. Mutation Research v. 636, p. 95-133, 2007.

MARGUI, E.; IGLESIAS, M.; QUERALT, I.; HIDALGO, M. Precise and accurate determination of lead isotope ratios in mining wastes by ICP-QMS as a tool to identify their source. Talanta 73, p. 700–709, 2007.

MASTRAL, A. M., DE LA CRUZ, M. T., LABORDA, F. Study of Pb sources by Pb isotope ratios in the airborne PM_{10} of Zaragoza, Spain. Journal of Environmental Monitoring, 2052-2057, 2009.

MELO, S. M. A. Formação Rio Claro e Depósitos Associados: Sedimentação

Neocenozóica na Depressão Periférica Paulista. São Paulo, 144 f. (Tese de Doutoramento) - Instituto de Geociências/USP – São Paulo, 1995.

MIRLEAN, N.; ROBINSON, D.; KAWASHITA, K.; LIDIA V.; CONCEIÇÃO, R.; CHEMALE, F. Identification of local sources of lead in atmospheric deposits in an urban area in Southern Brazil using stable lead isotope ratios. Atmospheric Environment, Volume 39, Issue 33, p. 6204-6212, 2005.

MONNA, F.; LANCELOT, J.; CROUDACE, I.W.; CUNDY, A.B.; LEWIS, J.T. Lead isotopic composition of airborne material from France and the Southern U.K. implications for Pb pollution sources in urban areas. Environmental Science & Technology, 31 pp. 2277–2286, 1997.

MUKAI, H.; FURUTA, N.; FUJII, T.; AMBE, Y.; SAKAMOTO, K.; HASHIMOTO, Y. Characterization of sources of lead in the urban air of Asia using ratios of stable lead isotopes. Environmental Sciences & Technology 27, 1347–1356, 1993.

NELMS, S., QUÉTEL, C., PROHASKA, T., VOGL, J., TAYLOR, P. Evaluation of detector dead time calculation models for ICP-MS. J. Anal. At. Spectrom.,16, 333-338, 2001.

OLIVEIRA, J. B.; CAMARGO, M. N.; ROSSI, M.; CALDERANO FILHO, B. Mapa pedológico do Estado de São Paulo. Campinas: Instituto Agronômico 4 mapas. Escala 1:500.000, 1999.

PENTEADO, M. M. Geomorfologia do setor centro-ocidental da depressão periférica paulista. Instituto de Geografia - USP. Série Teses e Monografias, n.22, 86 f, 1976.

POPE, C.A.; DOCKERY, D.W.; SCHWARTZ, J. Review of epidemiological evidence of health-effects of particulate air pollution. Inhalation Toxicology 7, 1–18, 1995.

POPE, C. A. Lung cancer, cardiopulmonary mortality, and long-term exposure to fine particulate air pollution. Journal of the American Medical Association v. 287, p. 1132-1141, 2002.

SALCEDO, D.; CASTRO, T.; BERNAL, J. P.; ALMANZA-VELOZ, V.; ZAVALA, M.; GONZÁLEZ-CASTILLO, E.; SAAVEDRA, M. I.; PEREZ-ARVÍZU, O.; DÍAZ-TRUJILLO, G. C.; MOLINA, L. T. Using trace element content and lead isotopic composition to assess sources of PM in Tijuana, Mexico. Atmospheric Environment, Volume 132, p. 171-178, 2016.

SCHWARTZ, J., DOCKERY, D.W., NEAS, L.M. Is daily mortality associated specifically with fine particles? Journal of Air and Waste Management Association 46, 927–939, 1996.

SETTLE, D.M., PATTERSON, C.C. Eolian inputs of lead to the South Pacific via rain and dry deposition from industrial and natural sources. Cosmochimica Acta, Spec. Pub. No., 3 (eds, H. P.Taylor, J. R. O'Neil, and I. R. Kaplan) 3, 285–294, 1991.

SILVA, A. A.; DE CASTRO, S. Solos de Goiás. Estado Ambiental de Goiás, 2002.

SKOOG, D., LEARY, J. Instrumentelle Analytik. Grundlagen, Geräte, Anwendung. Springer, Berlin 1996.

SOUZA DE LIMA, C. Determinação da Composição Isotópica de Chumbo e Estrôncio em Petróleo e Derivados. Dissertação de Mestrado. Universidade Federal do Pará. Instituto de Geociências. Programa de Pós-Graduação em Geologia e Geoquímica como Ferramenta para o Monitoramento Ambiental. Belém, 2010.

STURGES, W.T.; BARRIE L.A. The use of stable lead 206/207 ratios and elemental composition to discriminate the origins of lead in aerosols at a rural

site in Eastern Canada. Atmospheric Environment, 23, pp. 1645–1657, 1989.

TAYLOR, H. E. Inductively Coupled Plasma-Mass Spectrometry. Academic Press, San Diego 2001.

THOMAS, R. Practical Guide to ICP-MS. Dekker, New York, 2004.

TROPPMAIR, H. Atlas da qualidade ambiental e de vida de Rio Claro-SP. Instituto de Geociências e Ciências Exatas/UNESP, 72 f, 1992.

U.S. EPA - UNITED STATES ENVIRONMENTAL PROTECTION AGENCY. Air Quality Criteria for Particulate Matter. Draft Report, n°. EPA/600/P-99/002Af, United States, Oct. 2004.

VERON, A.; FLAMENT, P.; BERTHO, M.L.; ALLEMAN, L.; FLEGAL, R.; HAMELIN, B. Isotopic evidence of pollutant lead sources in Northwestern France Atmos. Env., 33, pp. 3377–3388, 1999.

WANG, S.Q.; ZHANG, J.L. Blood lead levels in children, China. Environmental Research 101, 412e418, 2006.

WIDORY, D.; ROY, S.; LE MOULLEC, Y. The origin of atmospheric particles in Paris: a view through carbon and lead isotopes. Atmospheric Environment, 38, 953–961, 2004.

WHO – WORLD HEALTH ORGANIZATION. Air Quality Guidelines for Particulate Matter, Ozone, Nitrogen Dioxide and Sulphur Dioxide. Global update 2005. Summary of Risk Assessment. Geneva, 2006.

WHOLGATE, S. T.; SAMET, J. M.; KOREN, H. S.; MAYNARD, R. L. Air Pollution and Health. San Diego: Academic Press, 1999.

XU, J.J.; CAO, K.F.; HOA, H.; DING, Y.M. Lead concentrations in fine particulate matter after the phasing out of leaded gasoline in Xi'an, China. Atmospheric Environment, Volume 46, January 2012, Pages 217-224, 2011.

ZAR, J. H. Biostatistical Analysis, Fourth Edition. Prentice-Hall International (UK) Limited. London. 1999

ZHENG, J., TAN, M., SHIBATA, Y., TANAKA, A., LI, Y. Characteristics of lead isotope ratios and elemental concentrations in PM_{10} fraction of airborne particulate matter in Shanghai after the phase-out of leaded gasoline. Atmospheric Environment, 1191–1200, 2004.